

**PERFORMANCE STUDY FOR GUIDANCE OF A  
GENERIC MISSILE USING FLOW EFFECTOR ON THE NOSE**

**PREPARED FOR**

**DEFENCE R&D CANADA - VALCARTIER  
R&D POUR LA DÉFENSE CANADA - VALCARTIER  
QUEBEC, QC G3J-1X5 CANADA  
Contract No. : W7701-0-2687/001/QCA  
Nicolas Hamel, Scientific authority  
Tel : 418-844-4000 ext. 4663**

**by**

**P.-A. Rainville  
P. Gosselin**



**NUMERICA TECHNOLOGIES INC.  
3420 Lacoste Street  
Québec, QC G2E 4P8 Canada**

**march/mars 2004**

**PERFORMANCE STUDY FOR GUIDANCE OF A  
GENERIC MISSILE USING FLOW EFFECTOR ON THE NOSE**

**PREPARED FOR**

**DEFENCE R&D CANADA - VALCARTIER  
R&D POUR LA DÉFENSE CANADA - VALCARTIER  
QUEBEC, QC G3J-1X5 CANADA  
Contract No. : W7701-0-2687/001/QCA  
Nicolas Hamel, Scientific authority  
Tel : 418-844-4000 ext. 4663**

**by**

**P.-A. Rainville  
P. Gosselin**



**NUMERICA TECHNOLOGIES INC.  
3420 Lacoste Street  
Québec, QC G2E 4P8 Canada**

**march/mars 2004**

**ABSTRACT/RÉSUMÉ**

Because of the high costs associated with flight and experimental measurements in wind tunnels and test cells, Computational Fluid Dynamics (CFD) is becoming a useful tool for predicting fluid flow. With the recent performance improvements of computers and numerical codes, a much faster prediction of fluid flow, shock wave position and aerodynamic coefficients calculation is believed to be possible allowing the simulations of more complex flow.

This report lies in the continuity of exploring phases on the feasibility to use Flow Effectors for Active Flow Control for the Guidance of Missiles. The present study is done on an aerodynamic geometry with a conical nose adapted to the wind tunnel model. Different combinations of rectangular flow effectors place on the nose can have very different characteristics in steady and unsteady operation. Each one of these items has a direct impact on the general performance of the missile. The missile performances can also be affected by flight parameters such as Mach number, altitude and angle of attack.

The aim of this study is to evaluate the performance of an active flow control in the form of a rectangular flow disturber with the aim of controlling a missile. Using CFD, combinations of different dimensions of flow effectors at different positions on the surface of the missile were evaluated for their impact on overall system performance for a missile flying at Mach 1.5 at an altitude of 6 km from zero to twenty degrees of angle of attack.

---

En raison des coûts élevés associés aux essais en vol et aux tests expérimentaux en soufflerie, les codes numériques de mécanique des fluides sont devenus des outils très utiles pour prédire les écoulements. Avec les récents développements dans le domaine de l'informatique et des codes numériques, une prédiction beaucoup plus rapide de l'écoulement, de la position, de la propagation des ondes de choc et de l'évaluation des coefficients aérodynamiques est rendue possible, permettant ainsi la simulation de problèmes plus complexes.

Ce rapport est en continuité de deux phases d'exploration sur la possibilité d'utiliser des perturbateurs d'écoulement pour le Contrôle Actif d'Écoulement pour le Guidage des Missiles. La présente étude est exécutée sur une géométrie aérodynamique avec un nez conique adaptée au modèle de la soufflerie. Différentes combinaisons de perturbateurs rectangulaires localisés sur le nez peuvent avoir différentes caractéristiques en régime permanent et transitoire. Chacun de ces items a un impact direct sur la performance générale du missile. Les performances du missile peuvent aussi être affectées par les paramètres de vol tels que le nombre de Mach, l'altitude et l'angle d'attaque.

Le but de cette étude est d'évaluer le rendement d'un contrôle actif d'écoulement sous forme d'un perturbateur rectangulaire, afin de contrôler la trajectoire d'un missile ou une fusée au moyen d'un Contrôle Actif d'Écoulement. En utilisant un code numérique de mécanique des fluides, différentes dimensions de perturbateurs avec différentes positions sur la surface du missile ont été évaluées afin de vérifier leur impact sur les performances globales d'un missile volant à Mach 1.5 à une altitude de 6 km, de zéro à vingt degrés d'angle d'attaque.

## TABLE OF CONTENTS

ABSTRACT/RÉSUMÉ.....	I
TABLE OF CONTENTS.....	II
LIST OF FIGURES .....	III
LIST OF TABLES .....	IV
NOMENCLATURE.....	V
ACKNOWLEDGMENTS .....	VI
EXECUTIVE SUMMARY.....	VII
1.0 INTRODUCTION.....	1
2.0 METHODOLOGY .....	2
2.1 MODELS .....	2
2.2 GRIDS.....	2
2.3 BOUNDARY CONDITIONS.....	3
2.4 AERODYNAMIC COEFFICIENTS .....	3
3.0 CALCULATIONS.....	5
3.1 FLOW EFFECTORS DIMENSIONS .....	5
3.2 POSITION OF FLOW EFFECTORS .....	6
3.3 RESULTS WITHOUT FLOW EFFECTORS .....	7
3.4 RESULTS WITH FLOW EFFECTORS .....	9
3.5 PARAMETRIC STUDY WITH FLOW EFFECTORS .....	11
4.0 CONCLUSION.....	13
5.0 REFERENCES.....	14
APPENDIX A - MESH FIGURES WITH RECTENGULAR FLOW EFFECTORS	
APPENDIX B - FLUENT™ SOLUTION FIGURES WITH RECTANGULAR FLOW EFFECTORS	
APPENDIX C - GRAPH OF THE PERFORMANCE OF RECTANGULAR FLOW EFFECTORS	

## LIST OF FIGURES

Figure 1: Coordinate system for the calculation of the aerodynamic coefficients and moment.....	4
Figure 2: Body alone geometry configuration with the 3D coordinate axis .....	5
Figure 3: Dimensions of the FE given in inches units. ....	6
Figure 4: Position of the baseline FE on the aerodynamic geometry.....	6
Figure 5: Position of the 3x FE on the aerodynamic geometry.....	7
Figure 6: Position of the 5x FE on the aerodynamic geometry.....	7

## APPENDIX A

- Figure A-1 View of the mesh in the far field and boundary conditions position
- Figure A-2 Zoomed view of the mesh around the baseline FE
- Figure A-3 Boundary refinement around the baseline FE
- Figure A-4 Block construction around the baseline FE
- Figure A-5 Block construction around the 3x FE
- Figure A-6 Block construction around the 5x FE
- Figure A-7 Mesh cut around the 3x FE in the X-Z plane
- Figure A-8 Mesh cut around the 3x FE in the Y-Z plane

## APPENDIX B

- Figure B-1 Pressure field in the plane of the angle of attack with three 5x FE at 10° AOA
- Figure B-2 Pressure field in the plane of the three 5x FE at 10° AOA
- Figure B-3 Mach number around 3 baseline FE with 30 degrees between them with 20° AOA
- Figure B-4 Mach number around 5 baseline FE with 15 degrees between them with 20° AOA
- Figure B-5 Mach number around 3 3x FE with 30 degrees between them with 15° AOA
- Figure B-6 Mach number around 3 3x FE with 30 degrees between them with 20° AOA
- Figure B-7 Pressure around 3 3x FE with 30 degrees between them with 15° AOA
- Figure B-8 Pressure around 3 3x FE with 30 degrees between them with 20° AOA
- Figure B-9 Dynamic pressure in the middle of the missile (0,2 m) with 15° AOA in the calculation with 3 3x FE having an angle of 30 degrees between them
- Figure B-10 Dynamic pressure in the middle of the missile (0,2 m) with 20° AOA in the calculation with 3 3x FE having an angle of 30 degrees between them
- Figure B-11 Mach number around a 5x FE with 0° AOA

## APPENDIX C

- Figure C-1 Graph of the performance of the baseline FE vs the angle of attack
- Figure C-2 Graph of the performance of the 3x FE vs the angle of attack
- Figure C-3 Graph of the performance of the 5x FE vs the angle of attack
- Figure C-4 Graph of the performance of the baseline FE vs the angle between the FE for an angle of attack is 10 degrees. The number of FE is limited to three. With an angle between the devices of zero degrees, there is only one FE.
- Figure C-5 Graph of the performance of the baseline FE vs the number of FE having an angle of 15 degrees between them and at an angle of attack of 10 degrees

**LIST OF TABLES**

Table 1	Reference values for the calculation of the aerodynamic coefficients.....	4
Table 2	Numerical configuration without FE .....	8
Table 3	Numerical coefficients results without FE .....	8
Table 4	Error between numerical results Missile Datcom 97™ results.....	8
Table 5	Numerical configuration with FE.....	9
Table 6	Results of the performance of the FE system.....	10

## NOMENCLATURE

$A$	Characteristic area	$m^2$
$h$	Enthalpy	J/kg
$L$	Characteristic length	m
$L_w$	Height of the first cells near the wall	m
$Ma$	Mach number	-
$P$	Pressure	Pa
$V$	Velocity	m/s
$V_w$	Velocity at the first cell near the wall	m/s
$T$	Temperature	K
$Y^+$	Near wall mesh refinement parameter	
$\rho$	Density	$kg/m^3$
$\rho_w$	Density at the first cell near the wall	$kg/m^3$
$\mu$	Viscosity	$kg/m\ s$
$\mu_w$	Viscosity at the first cell near the wall	$kg/m\ s$
DRDC	Defence Research & Development Canada	
CFD	Computational Fluid Dynamic	
CFL	Courant-Freidrich Lewis number	
AOA	Angle of attack	
MEMS	Micro Electro-mechanic systems	
FE	Flow effectors	

## ACKNOWLEDGMENTS

This project would not have been possible without the financial support of the Work Breakdown Element 13eg16 from the Technology Investment Fund of Defence Research and Development Canada. Special thanks to M. Nicolas Hamel from DRDC Valcartier for his advice and support during this project and M. Frank Wong from DRDC Valcartier for the administrative part.

## EXECUTIVE SUMMARY

The DRDC Valcartier Flight Mechanics Group is responsible for research in aerodynamic and flight dynamic behaviour of weapon systems. The aeroballistic facilities are being used to obtain aerodynamic coefficients necessary to perform trajectory simulations and for optimization of particular shapes of projectile or munitions to obtain the desired aerodynamic performance. To overcome some of the physical or financial constraints imposed by these experiments, a Computational Fluid Dynamics (CFD) approach can be used to complement and enhance experimental results.

The objective of the contract was to evaluate the performance of an active flow control in the form of a rectangular flow disturber with the aim of controlling a missile or rocket. Using CFD, combinations of different dimensions of flow effectors at different positions on the surface of the missile were evaluated for their impact on overall system performance for a missile flying at Mach 1.5 at wind tunnel conditions from zero to twenty degrees of angle of attack.

A series of CFD analysis were made on an aerodynamic geometry with some Flow Effectors. Three different dimensions of rectangular Flow Effectors were evaluated for their side force performance. The side force generated by the Flow Effectors should be able to steer a missile. For the baseline flow effectors, two configurations were analysed. A configuration with three 3x Flow effectors were calculated and two configurations with five times the baseline Flow Effectors were calculated. The Flow effectors were located in a perpendicular plane with the angle of attack. The experience gained during the previous work was used as a guideline for determining the models and setting. The validation was done in a previous work about the MEMS feasibility [DeChamplain et al. (2002)]. Finally, recommendations for improvements of the performance were stated.

This project was part of DRDC technology investment found (TIF) project "Supersonic Missile Flight Control by Manipulation of the Flow Structure using Micro-Actuated Surfaces". It resulted in an improved capability to predict numerically the aerodynamic behaviour of rectangular Flow Effectors before they can be tested in DRDC Valcartier wind tunnel.

## 1.0 INTRODUCTION

Flow effectors (FE) are integrated devices located in strategic places on the surface of a missile. These systems can control and actuate on the micro scale, and function individually or in arrays to generate effects on the macro scale. In the most general form, MEMS consist of mechanical microstructures, micro sensors, micro actuators and electronics integrated in the same environment (i.e. on a silicon chip). Miniaturization of mechanical systems promises unique opportunities for new directions of scientific and technological progress.

Missile guidance permits an increase in lethality for combat superiority. The performance of this system is function of the execution quality of this command. The majority of missiles use aerodynamic surfaces to accomplish this work. The control of the thrust vector constitutes another strategy for missile control. Nevertheless, these systems require a structure and an actuator. This implies number of systems to accomplish the task, which reduces the reliability and increases the weight of the mechanism. Aerodynamic surfaces need a relatively important space for storage. Depending on the desired result, one might wish to delay or accelerate transition, reduce drag, or increase manoeuvrability. Removing conventional controls could lead to significant weight reductions or decrease the missile signature.

The present work analyses different types of flow effectors, which are placed in a perpendicular plane with the angle of attack. In the previous work with MEMS, [DeChamplain et al. (2001)] and [DeChamplain et al. (2002)], MEMS devices were located in the same plane of the angle of attack. Because the missile when at an angle of attack hid the MEMS, its performance was found to be relatively low. A general objective of research about MEMS is to investigate the magnitude and type of surface deformation necessary on the surface of a missile or rocket to obtain sufficient control authority for effective guidance during flight. This project was part of DRDC technology investment found (TIF) project "Supersonic Missile Flight Control by Manipulation of the Flow Structure using Micro-Actuated Surfaces".

The aim of this study was achieved by a Computational Fluid Dynamics (CFD) analysis. The commercial CFD code Fluent™ was used to accomplish these calculations. One should note that the mesh for every CFD simulation was generated with the commercial code Gambit™. The methodology used included many steps. The experience gained during the previous work [DeChamplain et al. (2002)] was used as a guideline. In the previous work, a good validation step was done for the geometry without MEMS.

This document is divided in many parts. At first, details are given about the grid and the model used in the previous work. Furthermore in the second part, a description of the flow effectors, their positions, their dimensions and the different angles of attack that were used are described. Presentation of the results was done accordingly. In the third part, an analysis of the results is given and a discussion is presented. Finally, a conclusion and suitable recommendations are given in the last section.

## 2.0 METHODOLOGY

When a Computational Fluid Dynamics (CFD) study is to be done, a complete validation study must be undertaken. Basically, this means that CFD results must be verified by comparing them with experimental data, to be sure that the CFD model can predict correctly all the physical phenomena's. In the previous study on MEMS [DeChamplain et al. (2002)] a good validation case was done. The present work is based on the experience gained in the past. The information about the various models available in Fluent™ will not be given in this report. Nonetheless, it could be useful to indicate briefly some parameters that were selected for the present simulations. Additionally, a validation is done with a mesh that is refined in the boundary layer.

### 2.1 Models

Within Fluent™ it is necessary to set many parameters for calculation purposes. All the possibilities will not be described here. Only parameters chosen for the present analysis will be mentioned. Readers who would like more details about those parameters should consult [DeChamplain et al. (2001)] or Fluent™ literature.

In the present simulations, Navier-Stokes equations are resolved with the coupled form of the code where the energy equation is solved simultaneously with the fluid equations. Those equations are solved with an explicit pseudo-time formulation. This formulation calculates more rapidly and need less computer memory. The k-ε model improved with the Realizable model is adopted to take into account turbulence and vortex formation. Finally, the effects of boundary layer are evaluated with the Enhanced-Wall treatment model. This model proposes two options to improve the calculation. The pressure one is active, but since the thermal heat transfer is not calculated, the thermal option is not activated. The working fluid is air. The density is calculated with the ideal-gas law and the viscosity, with the Sutherland three coefficients model. All the other properties are as the default settings.

### 2.2 Grids

In the present study it is not possible to split the calculation domain in two parts like it was done in the previous work [DeChamplain et al. (2002)]. Since the Flow effectors (FE) are located in a perpendicular plane with the angle of attack, the symmetry plane that existed in the previous work disappeared in this case. The complete domain was calculated in the present 3D calculation. As the present geometry had a small rounded nose, it was easier to build mesh upstream of the geometry. A small cylinder was built starting from the nose to the upstream part of the domain. The diameter of the cylinder was around 0,003 inches compared to the 0,005 inches round tip of the nose reducing the mesh skewness on the nose tip.

In accordance with the previous MEMS study, grids generated were structured. It has been demonstrated that an unstructured mesh shows instabilities and cannot give reasonable solutions. However, some differences exist in the mesh employed presently. All of them are related to rectangular flow effectors that needed some refinement in the grid in their vicinity. Since the Enhanced-Wall treatment was used, the mesh had to have a  $Y^+$  parameter around 1 over all the missile wall. The supersonic shock wave presence makes it difficult to establish the  $Y^+$  with the same value over the entire missile. An effort was made to have a more favourable  $Y^+$  on the Flow effectors (FE) device and region. In the results tables, the  $Y^+$  is calculated over the entire missile and around the FE region. It is to be considered as a mean  $Y^+$ . It may be important to remember that the  $Y^+$  parameter is

calculated like a Reynolds number at the first cell near the wall. Equation (1) is used to calculate the  $Y^+$  value. This value is normally calculated by Fluent™ code. This equation includes density  $\rho_w$ , velocity  $V_w$ , height of the first cells  $L_w$  and viscosity  $\mu_w$ . All those values are calculated at the first cell near the wall.

The Flow effectors (FE) analysed in the present study had the shape of a rectangular effectors. Three FE were analyzed, the baseline effectors, the three time baseline effectors and the five time baseline effectors. The relative position and number of FE were the parameters of interest for each FE dimension. The calculation included 1, 3 or 5 FE. All FE were located at 25,32 mm (0,997 inches) from the nose tip. The space between the FE was defined by an angle around the axis of the geometry. The angle between the FE was 15 or 30 degrees and for the 3 FE geometries, the angle was 45 degrees. The angles of attack for the study were 0, 10, 15 and 20 degrees.

A view of the mesh in the far field is presented in figure A-1. Details of the refinement necessary around the FE are presented in figures A-2 and A-3 with the baseline FE. To simplify the meshing around the FE, the domain was split into volumes. Structured volumes are presented in figure A-4 for the baseline FE, in figure A-5 for the 3x FE and in figure A-6 for the 5x FE. Finally, figures A-7 and A-8 give an example of the mesh around the 3x FE. Figures A-1 to A-8 are presented in appendix A.

$$Y^+ = \frac{\rho_w V_w L_w}{\mu_w} \quad [1]$$

### 2.3 Boundary Conditions

The domain is surrounded by a pressure far-field boundary condition in front and around the calculation domain. The outlet of the domain determined by a pressure outlet boundary condition to reduce the boundary condition effect and to be sure that no shock wave reflection can exist. The missile is flying according to new conditions compared to the previous MEMS study. The missile has a design Mach number of 1,5. The static temperature is 206 K and the static pressure is 26 000 Pa. Furthermore, three angles of attack (AOA) were selected for calculations: 10 and 15 degrees. Angle of attack of 0 and 20 degrees were kept as an option if time permitted.

### 2.4 Aerodynamic Coefficients

The results presented will the aerodynamic coefficients. The aerodynamic coefficients are calculated with the missile coordinate axis. The origin of the coordinate axis is located at the nose tip. The aerodynamic moment is calculated at the base of the missile. Figure 1 presents the coordinate system for the aerodynamic coefficients and the moment center for the moment calculation. The base drag is not calculated in the x axis aerodynamic coefficient. Table 1 presents the reference values used in the calculations.

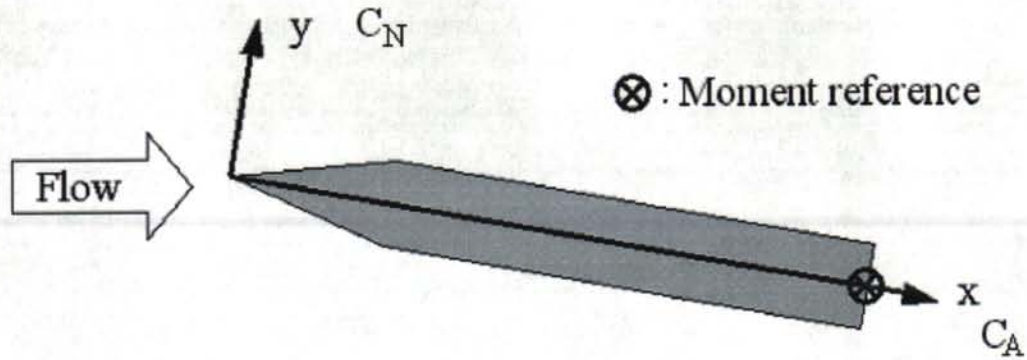


Figure 1: Coordinate system for the calculation of the aerodynamic coefficients and moment.

Area ( $A$ ), $m^2$	706,9 E-6	Temperature ( $T$ ), K	206
Density ( $\rho$ ), $kg/m^3$	0,439 7104	Velocity ( $V$ ), m/s	431,423
Enthalpy ( $h$ ), J/kg	300 387,8	Viscosity ( $\mu$ ), kg/m s	1,789 E-5
Length ( $L$ ), m	0,03	Ratio of specific heats	1,4
Pressure ( $P$ ), Pa	26 000		

TABLE 1 REFERENCE VALUES FOR THE CALCULATION OF THE AERODYNAMIC COEFFICIENTS

### 3.0 CALCULATIONS

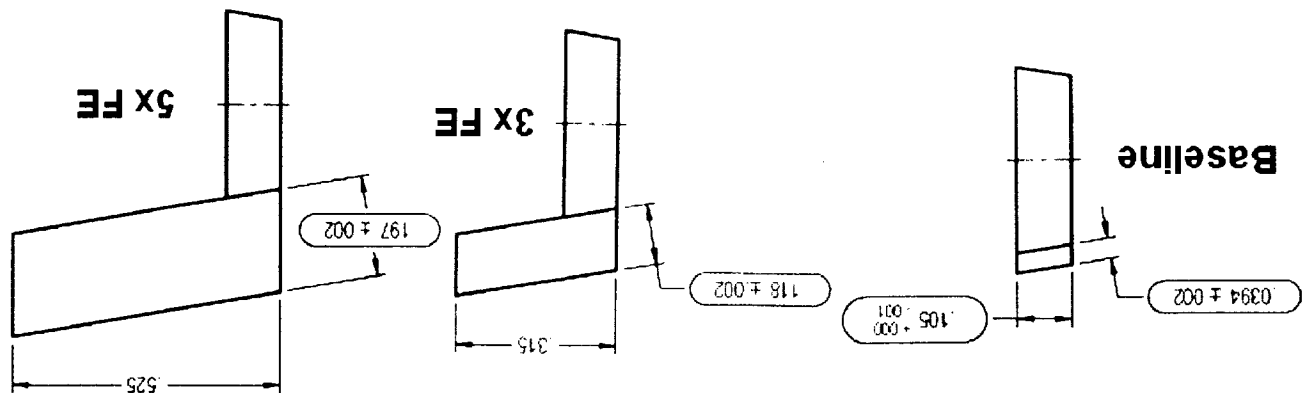
To evaluate the effect of the FE on the flow and the accuracy of the calculation, the body alone geometry was simulated at every angle of attack. The results were compared with Missile Datcom 97™ results to have an idea of the length scale of the solution. The Missile Datcom 97™ calculation had a difference of around 25% with the wind tunnel results. The body alone geometry is shown in figure 2. As presented in figure 1, the x axis is on the centre axis of the geometry. The angle of attack is in the X-Y plane and the FE devices are located on the positive Z side of the geometry. The diameter of the geometry is 30 mm. The conical part of the geometry is 90 mm in length and the cylindrical part is 300 mm in length. The total length of the geometry is 390 mm (15,353 inches).



Figure 2: Body alone geometry configuration with the 3D coordinate axis

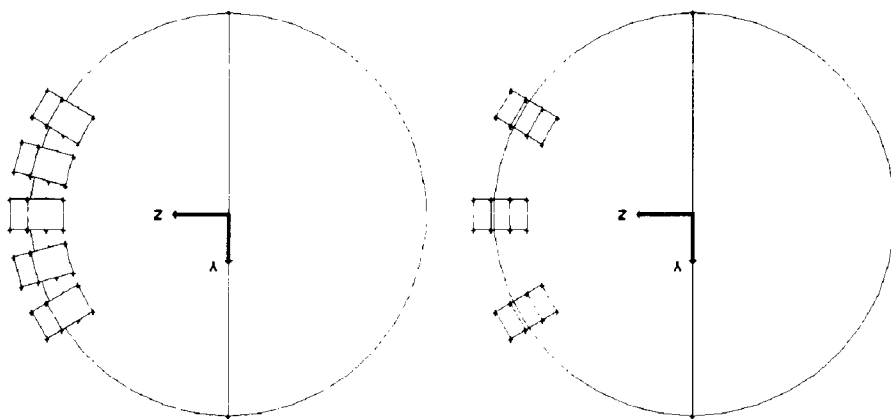
#### 3.1 Flow effectors dimensions

The Flows effectors (FE) dimensions are simpler compared to the microbubbles of [DeChamplain et al. (2002)]. The length of the FE was defined in the x axis of the aerodynamic geometry. The width of all FE is 0,78 mm (0,031 inches). The baseline FE was approximately 1 mm (0,0394 in) high and 2,67 mm long (0,105 in). The three time baseline (3x) FE were near 3 mm by 8 mm (0,118 in by 0,315 in) and the five time baseline (5x) FE were around 8 mm by 13,3 mm or (0,197 in by 0,515 in). The exact dimensions of all FE are presented in figure 3. The FE dimensions are all defined in inches on the figures.



### 3.2 Position of Flow effectors

In the study only some configurations were simulated for every angle of attack. For the baseline flow effectors (FE), the simulation was made with 3 FE having an angle of 30 degrees between each one of them. The 5 FE had an angle of 15 degrees between each one of them. Only the configuration with 3 FE having an angle of 30 degrees between the effectors was calculated for the 3x FE. The configurations with 1, 3 and 5x FE having an angle of 45 degrees between them were the last ones to be calculated. Three other configurations with an angle of attack of 10 degrees using the baseline FE were done. The configurations were with 1 FE, 3 FE having an angle of 15 degrees between the devices and 3 FE having an angle of 45 degrees between the devices. Those three calculations permitted to build a small parametric study with the number of effectors and the angle between them. Figure 4 presents the configuration calculated with the baseline FE. Figure 5 shows the configuration calculated with the 3x FE. Figure 6 presents the configuration calculated with the 5x FE.



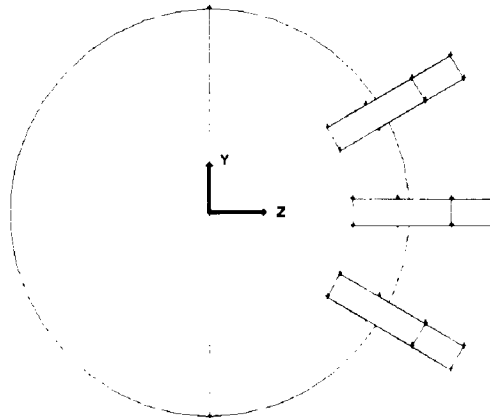


Figure 5: Position of the 3x FE on the aerodynamic geometry

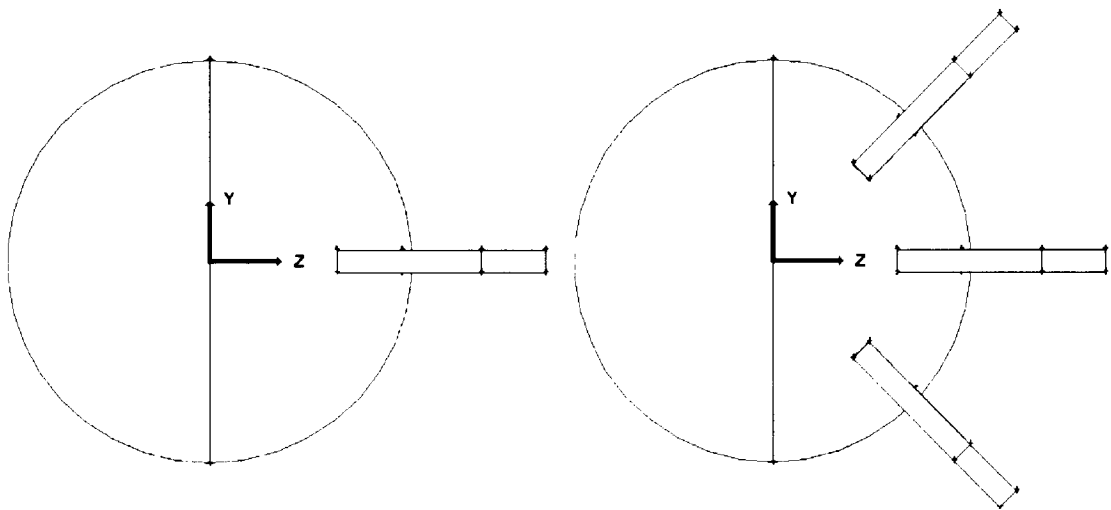


Figure 6: Position of the 5x FE on the aerodynamic geometry

### 3.3 Results without Flow effectors

To begin with, a calculation of the aerodynamic geometry was done to define a mesh having a  $Y^+$  parameter near one. The first mesh gave a  $Y^+$  value near 0,03 in the Flow effectors (FE) zone. With a too small value of  $Y^+$ , a second calculation presented a mean value of  $Y^+$  of 0,45 in the FE zone. Since no experimental data were available to verify the exactitude of the calculation when the study begun, it was decided to build another mesh to having a  $Y^+$  value more near of the ideal value of one. The last mesh had an  $Y^+$  mean value in the FE zone of 0,88. Along the strait part of the body, the flow is less aggressive on the geometry wall, and the calculated  $Y^+$  value is lower. The  $Y^+$  over all the aerodynamic geometry varied between 0,6 and 0,67 with an angle of attack. The height of the first cells was at  $1,5 \times 10^{-4}$  inches to obtain the actual  $Y^+$  value. The calculation for all the study included two values of  $Y^+$ . The first one was the mean value in the FE zone and the FE itself. The second one was the mean value over all the aerodynamic body and it included the FE itself for the calculation with the FE. Table 2 include the condition of the calculation without FE. Table 3 include the aerodynamic coefficients results for the calculation without the FE. The results for Missiles Datcom™ calculation are also included in the table. Without FE,  $C_Y$  should be zero; this value in the table gives an idea of the precision of the calculation. FE side force under the present value may represent a negligible effect of the FE.

UNCLASSIFIED/ SANS CLASSIFICATION

Name	Mesh			AOA
	Nb cells	Y+ (FE)	Y+ (All)	
Without FE				
Mis-CC_AOA00	893276	0,87	0,60	0
Mis-CC_AOA10	893276	0,88	0,64	10
Mis-CC_AOA15	893276	0,88	0,66	15
Mis-CC_AOA20	893276	0,88	0,67	20
Missile Datcom				
Datcom AOA00	---	---	---	0
Datcom AOA10	---	---	---	10
Datcom AOA15	---	---	---	15
Datcom AOA20	---	---	---	20

TABLE 2 NUMERICAL CONFIGURATION WITHOUT FE

Name	Forces			Moments		
	C <sub>x</sub>	C <sub>N</sub>	C <sub>Y</sub>	C <sub>l</sub>	C <sub>n</sub>	C <sub>m</sub>
<b>Without FE</b>						
Mis-CC_AOA00	0,2399	0,0000	0,0001	0,0000	0,0004	0,0001
Mis-CC_AOA10	0,2429	0,6601	0,0004	0,0000	0,0016	-5,7154
Mis-CC_AOA15	0,2309	1,3234	0,0087	-0,0001	0,0306	-10,6938
Mis-CC_AOA20	0,2084	2,5469	0,0512	-0,0001	0,2422	-19,4643
<b>Datcom</b>						
Datcom AOA00	0,2310	0,0000	0,0000	0,0000	0,0000	0,0000
Datcom AOA10	0,2027	0,9780	0,0000	0,0000	0,0000	4,8660
Datcom AOA15	0,1691	1,5760	0,0000	0,0000	0,0000	8,1840
Datcom AOA20	0,1238	3,2670	0,0000	0,0000	0,0000	19,4970

TABLE 3 NUMERICAL COEFFICIENTS RESULTS WITHOUT FE

AOA	Aerodynamic coefficient		
	C <sub>x</sub>	C <sub>N</sub>	C <sub>m</sub>
0	3,8%	---	---
10	19,8%	-32,5%	17,5%
15	36,5%	-16,0%	30,7%
20	68,3%	-22,0%	-0,2%

TABLE 4 ERROR BETWEEN NUMERICAL RESULTS MISSILE DATCOM 97™ RESULTS

### 3.4 Results with Flow effectors

Since the calculations without Flow effectors (FE) showed acceptable results, it was now possible to calculate the performance of the FE with good confidence. The results are included in two tables. Table 5 presents the calculation conditions and settings. This table includes the number of cells in the mesh and two mean  $Y^+$  values. The table includes FE numbers and their positions. Finally, the table presents the angle of attack of calculation. Table 6 includes the performance results as aerodynamic coefficients and moments.

Name	Mesh			Flow effectors		AOA
	Nb cells	Y+ (FE)	Y+ (All)	Number	type	
Baseline (FE)						
MisC-A1_AOA10	1129256	0,90	0,65	1	1	10
MisC-A2_AOA10	1125750	0,86	0,64	3	2x 15°	10
MisC-A3_AOA00	1125750	0,85	0,60	3	2x 30°	0
MisC-A3_AOA10	1125750	0,88	0,64	3	2x 30°	10
MisC-A3_AOA15	1125750	0,88	0,66	3	2x 30°	15
MisC-A3_AOA20	1125750	0,88	0,66	3	2x 30°	20
MisC-A4_AOA10	1104946	0,88	0,64	3	2x 45°	10
MisC-A5_AOA00	1293010	0,83	0,60	5	4x 15°	0
MisC-A5_AOA10	1293010	0,85	0,64	5	4x 15°	10
MisC-A5_AOA15	1293010	0,85	0,66	5	4x 15°	15
MisC-A5_AOA20	1293010	0,85	0,66	5	4x 15°	20
Three time baseline (3x FE)						
MisC-B3_AOA00	1142698	0,85	0,60	3	2x 30°	0
MisC-B3_AOA10	1142698	0,88	0,65	3	2x 30°	10
MisC-B3_AOA15	1142698	0,89	0,66	3	2x 30°	15
MisC-B3_AOA20	1142698	0,89	0,67	3	2x 30°	20
Five time baseline (5x FE)						
MisC-C1_AOA00	1300894	0,93	0,61	1	1	0
MisC-C1_AOA10	1300894	0,94	0,65	1	1	10
MisC-C1_AOA15	1300894	0,95	0,66	1	1	15
MisC-C1_AOA20	1300894	0,94	0,67	1	1	20
MisC-C4_AOA00	1385693	0,88	0,60	3	2x 45°	0
MisC-C4_AOA10	1385693	0,89	0,64	3	2x 45°	10
MisC-C4_AOA15	1385693	0,89	0,66	3	2x 45°	15
MisC-C4_AOA20	1385693	0,90	0,67	3	2x 45°	20

TABLE 5 NUMERICAL CONFIGURATION WITH FE

UNCLASSIFIED/ SANS CLASSIFICATION

Name	Results					
	$C_x$	$C_N$	$C_Y$	$C_l$	$C_n$	$C_m$
<b>Baseline (FE)</b>						
MisC-A1_AOA10	0,2450	0,6602	-0,0397	-0,0002	-0,1559	-5,7326
MisC-A2_AOA10	0,2463	0,6598	-0,0353	-0,0003	-0,1413	-5,7322
MisC-A3_AOA00	0,2428	0,0000	-0,0007	0,0000	-0,0052	-0,0001
MisC-A3_AOA10	0,2469	0,6617	-0,0777	-0,0003	-0,3137	-5,7475
MisC-A3_AOA15	0,2352	1,3415	-0,3439	-0,0006	-1,4170	-10,7895
MisC-A3_AOA20	0,2132	2,5928	-0,4648	-0,0017	-2,5391	-19,6688
MisC-A4_AOA10	0,2472	0,6634	-0,0998	-0,0003	-0,4025	-5,7509
MisC-A5_AOA00	0,2443	0,0000	-0,0012	0,0000	-0,0097	0,0000
MisC-A5_AOA10	0,2485	0,6596	-0,0362	-0,0004	-0,1509	-5,7308
MisC-A5_AOA15	0,2365	1,3250	-0,1586	-0,0005	-0,6230	-10,7189
MisC-A5_AOA20	0,2149	2,5637	-0,3107	-0,0012	-1,6377	-19,5481
<b>Three time baseline (3x FE)</b>						
MisC-B3_AOA00	0,2528	0,0000	-0,0021	0,0000	-0,0141	-0,0001
MisC-B3_AOA10	0,2584	0,6919	-0,2290	-0,0045	-1,0811	-6,0329
MisC-B3_AOA15	0,2469	1,3900	-0,5686	-0,0077	-2,9107	-11,2638
MisC-B3_AOA20	0,2268	2,5983	-0,4338	-0,0103	-3,1138	-20,0635
<b>Five time baseline (5x FE)</b>						
MisC-C1_AOA00	0,2490	0,0000	-0,0007	0,0000	-0,0003	-0,0001
MisC-C1_AOA10	0,2529	0,7118	-0,2566	-0,0107	-1,3651	-6,2976
MisC-C1_AOA15	0,2430	1,3947	-0,4430	-0,0177	-2,9600	-11,5818
MisC-C1_AOA20	0,2235	2,6862	0,0037	-0,0234	-2,0535	-20,7208
MisC-C4_AOA00	0,2638	0,0000	-0,0030	0,0000	-0,0199	-0,0002
MisC-C4_AOA10	0,2673	0,7385	-0,3901	-0,0144	-2,0864	-6,4674
MisC-C4_AOA15	0,2565	1,4580	-0,6996	-0,0237	-4,4060	-11,9883
MisC-C4_AOA20	0,2390	2,7342	-0,2779	-0,0338	-4,0068	-21,2730

TABLE 6 RESULTS OF THE PERFORMANCE OF THE FE SYSTEM

It is important to consider that a  $C_Y$  value, which is the side force of the FE device, that has a value below the calculations without FE has a negligible effect. Table 6 shows a negligible effect of the FE with an angle of attack of 0 degrees. With an angle of attack of 10 degrees, the side force was around one tenth of the drag for baseline FE. The side force was bigger than the drag for 5x FE. Normally the performance of the FE increases when the angle of attack increases. But, with an angle of attack of 20 degrees, the boundary layer was separating over the FE, reducing the side force of the devices. For the calculation with a 5x FE at 20 degrees of angle of attack, the side force effect was changing of side. Generally, side force applied on the missile by a FE stirred the missile in the opposite side of its original position.

Fluent™ solutions are presented on some contours in appendix B. Figures B-1 and B-2 present a general flow field with pressure contours in plane X-Y, with an angle of attack, and plane X-Z, with the FE. These two figures were from the 3x FE with an angle of attack of 10 degrees. The shock waves from the geometry with an angle of attack are easy to see in figure B-1. Effects of FE are presented in figure B-2. Figure B-3 shows the Mach number around three baselines FE and figure B-4 presents the Mach number around five baselines FE. These two figures help understanding why side force performance is lower when FE having an angle of 15 degrees between them. Figure B-4 shows

that the Mach number stays small between the FE. When the space between FE is increased, as in figure B-3, the flow can pass through all FE without being perturbed. A special effect was the performance lost that happened with the 3x FE and 5x FE at an angle of attack of 20 degrees. To understand this phenomenon, Mach number, static pressure field and dynamic pressure field were compared. Figures B-5 to B-10 compare solutions with 3x FE with an angle of attack of 15 degrees and 20 degrees. Mach number and static pressure fields were presented around the FE. Dynamic pressure field was captured at the half-length of the missile to see if the generated vortex was perturbed. Figures with Mach number contours present a high velocity over the upper FE with an angle of attack of 15 degrees. With an angle of attack of 20 degrees, a boundary layer separation occurred over the upper FE. A small vortex created a low velocity zone over the lower FE with an angle of attack of 15 and 20 degrees. These two phenomena's can explain the low side force at 20 degrees AOA. Static pressure around the two solutions had small differences. A pressure difference was calculated under the missile because of the effect of the variation of angle of attack. The boundary layer separation had the effect that the pressure stayed higher with an angle of attack of 20 degrees. The figure with the dynamic pressure contours shows that the 3x FE modified the vortex shape created by the missile. The difference between the two calculations were small and it did not appear to explain the lost of side force when the angle of attack was increased to 20 degrees. Finally, the flow field stayed very symmetric around the FE when the angle of attack was zero. Figure B-11 was calculated with three 5x FE. The small performance of the FE without an angle of attack could be explained by the fact that the FE were hidden by the shock wave and by the symmetric flow around the FE.

Three graphs were built for side force performance of the FE with an angle of attack. In those graphs, a side force is calculated from 15 degrees AOA on the missile with no flow effectors. This could be explained from the fact that the mesh is not equally distributed around the body of the missile and that small mesh distortions could induce asymmetrical vortices, which could induce a side force on the missile body. Figure C-1 presents the performance of a baseline FE. Figure C-2 presents the side force of 3x FE. For the 3x FE, we can see that the side force drops from 15 to 20 degrees AOA. This is explained by the fact that the upper flow effector is in a stall on its upper surface as seen in figures B-5 to B-8 in appendix B. Figure C-3 presents the performance of the 5x FE. With one 5x FE, the low side force performance can be explained by a boundary layer separation near the body of the missile. For the configuration with three FE, some vortex were generate at the tip of the FE. The vortex generated a low velocity region in the middle of the FE with an angle of attack of 15 and 20 degrees. The low velocity zone create by the vortex took a more important area with an angle of attack of 20 degrees, which explain the lower performance. On those graphs, side force is presented as a pushing effect on the missile to obtain positive value. Positive values are easier to compare the side force performance of the FE.

### 3.5 Parametric study with Flow effectors

With baseline Flow effectors (FE), some additional configurations were calculated. Those calculations permitted to understand the effect of the angle between FE and the number of FE. For those two parametric studies, the angle of attack was 10 degrees. In the first study, effect of the angle between FE was analysed. The results are presented on graphs C-4 in appendix C. Results show that when the angle between FE was increased, performance increased. But results also show that at an angle of 15 degrees between the FE was not enough to have an effect on side force performance. Side force approximately doubled from one FE when the FE had an angle of 30 degrees between them. The

UNCLASSIFIED/ SANS CLASSIFICATION

side force was 2,5 times bigger with FE having an angle of 45 degrees between them, than with only one FE.

The second parametric study concerned the number of FE. The FE that had an angle of 15 degrees between them made it easier the parametric study with this angle. The study compares the side force without FE, with one, three and five FE. Results are presented on graphs C-5 in appendix C. The graph presents a small variation of the side force with the number of FE.

#### 4.0 CONCLUSION

This study on flow effectors (FE) aimed at defining the influence of the number and the position of the FE on a missile body and the effect of the angle of attack. Furthermore, three dimensions of rectangular FE were analysed. It was desired to know if a given configuration for FE could have a greater impact than others. Since the validation was completed in previous work, the model selection was defined with the experience gained. From the results obtained with numerical simulations, some remarks can be given. First of all, the FE can achieve a better side force compared to the ones calculated in the previous work. The performance is very sensitive to the angle of attack. When the angle of attack is zero, the side force is near zero. The side force coefficient of the FE can be as two times the drag for baseline FE for an angle of attack of 20 degrees. The side force, for the 3x FE, is more than two times the drag at an angle of attack of 15 degrees, but the performance reduces when the angle of attack is increased to 20 degrees. The 5x FE also permits an important side force at an angle of attack of 15 degrees, but an important performance lost happen when the when the angle of attack is 20 degrees. For one 5x FE with an angle of attack of 20 degrees, the side force becomes near zero and the force is switching side. The FE creates an important force that can steer the missile in the opposite direction of its original position. In a future work, it will be interesting to have a more complete parametric study about the number of FE having a different angle between them. Another parametric study can be done to identify the effect of the dimensions of the FE and the optimal dimensions. The present study presents a good performance of the FE when they are placed in a perpendicular plane with an angle of attack. The previous work had resulted in a poor performance with the FE in the same plane with the angle of attack. Another question remains, what would be the performance of the FE with an intermediate plane with the angle of attack ?

## 5.0 REFERENCES

DeChamplain, A., Gosselin, P., Hamel, N., and Rainville, P.-A., "Feasibility of Active Flow Control with MEMS for Missile or Rocket Guidance.", Numerica Technologies Inc., July 2001, UNCLASSIFIED.

DeChamplain, A., Gosselin, P., Harrison, V., and Rainville, P.-A., "Feasibility of Missile Guidance using MEMS-Based Active Flow Control – Part 2", Numerica Technologies Inc., March 2002, UNCLASSIFIED.

Esenwein, F.T., Obery, L.J., and Schueller, C.F., "Aerodynamic Characteristics of NACA RM-10 Missile in 8 by 6 foot Supersonic Wind Tunnel at Mach Numbers from 1.49 to 1.98; II- Presentation and Analysis of Force Measurements". NACA Research Memorandum RM E50D28, July 1950.

Lesage, F., Boulianne, M.-A. "Navier-Stokes Prediction of Missile Flowfields with Wing and Body Vortices ", DREV-TM-9835, February 1999, UNCLASSIFIED.

T. Tsao, F. Jiang, R. A. Miller, Y. C. Tai, B. Gupta, R. Goodman, S. Tung, and C. M. Ho, "An Integrated MEMS System for Turbulent Boundary Layer Control," Technical Digest, 1997 International Conference on Solid-State Sensors and Actuators (Transducers '97), Chicago, IL, Vol. 1, pp. 315-318, Jun. 16-19 (1997).

## APPENDIX A

MESH FIGURES WITH  
RECTANGULAR FLOW EFFECTORS

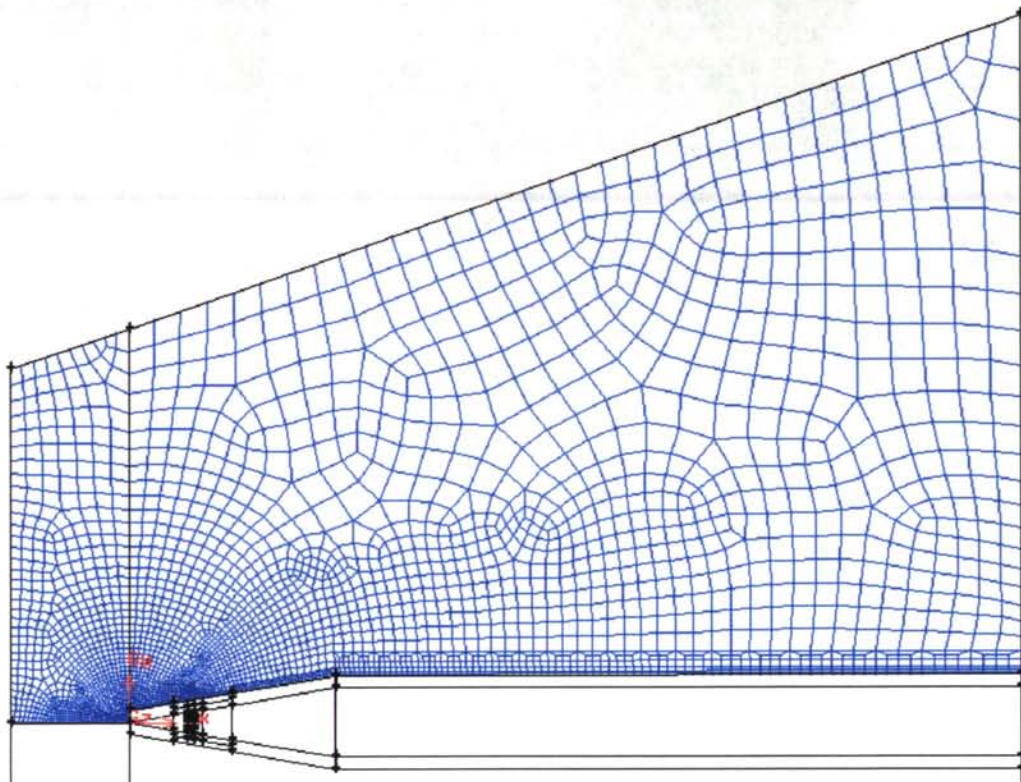


Figure A-1 View of the mesh in the far field and boundary conditions position

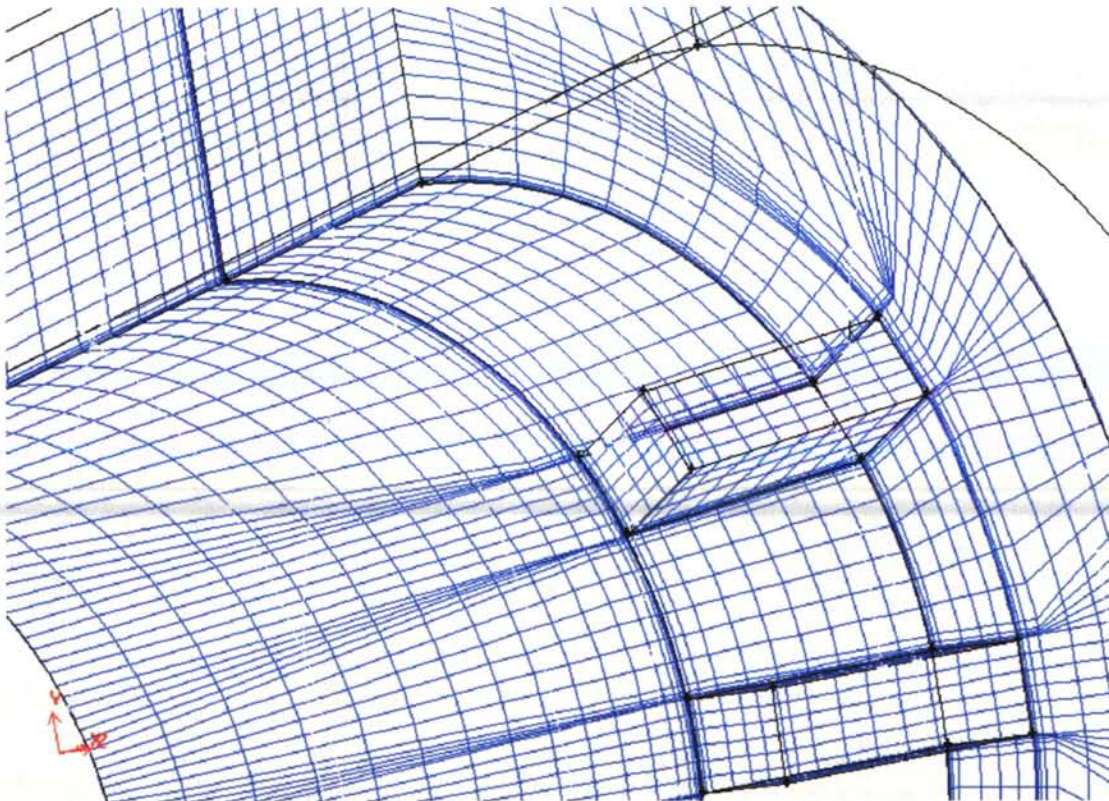


Figure A-2 Zoomed view of the mesh around the baseline FE

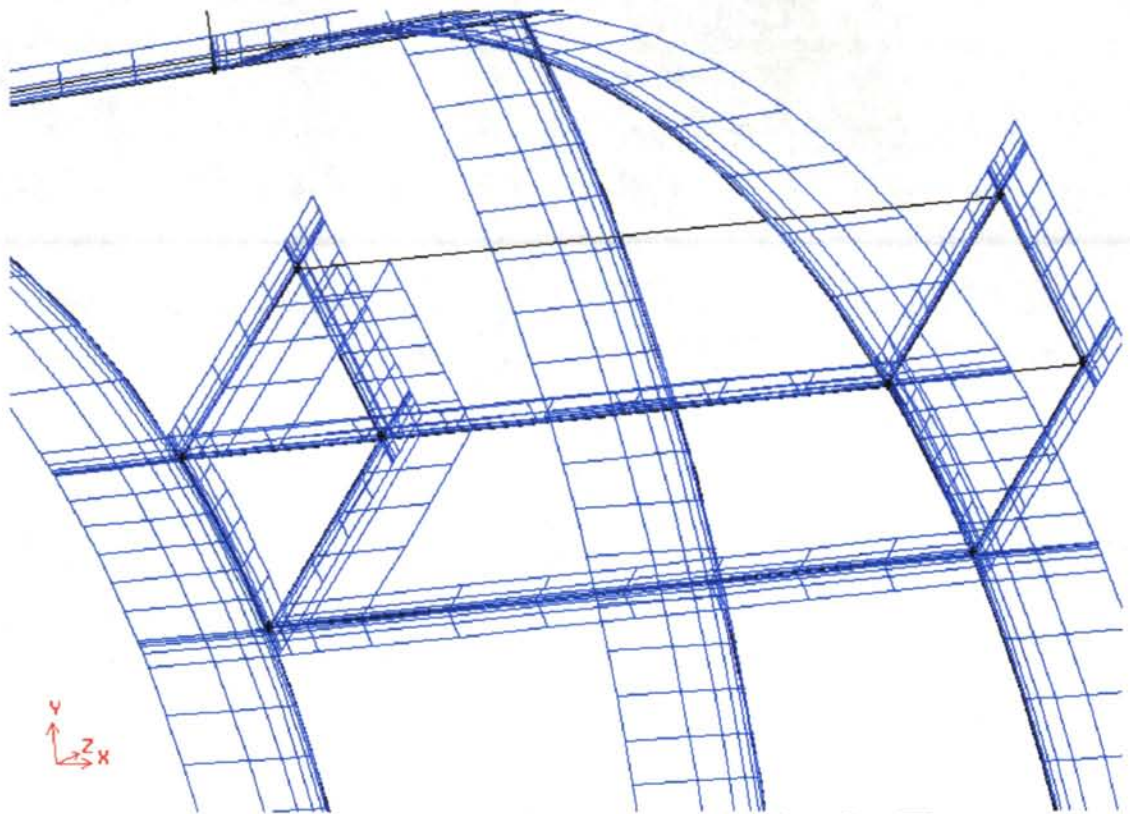


Figure A-3 Boundary refinement around the baseline FE

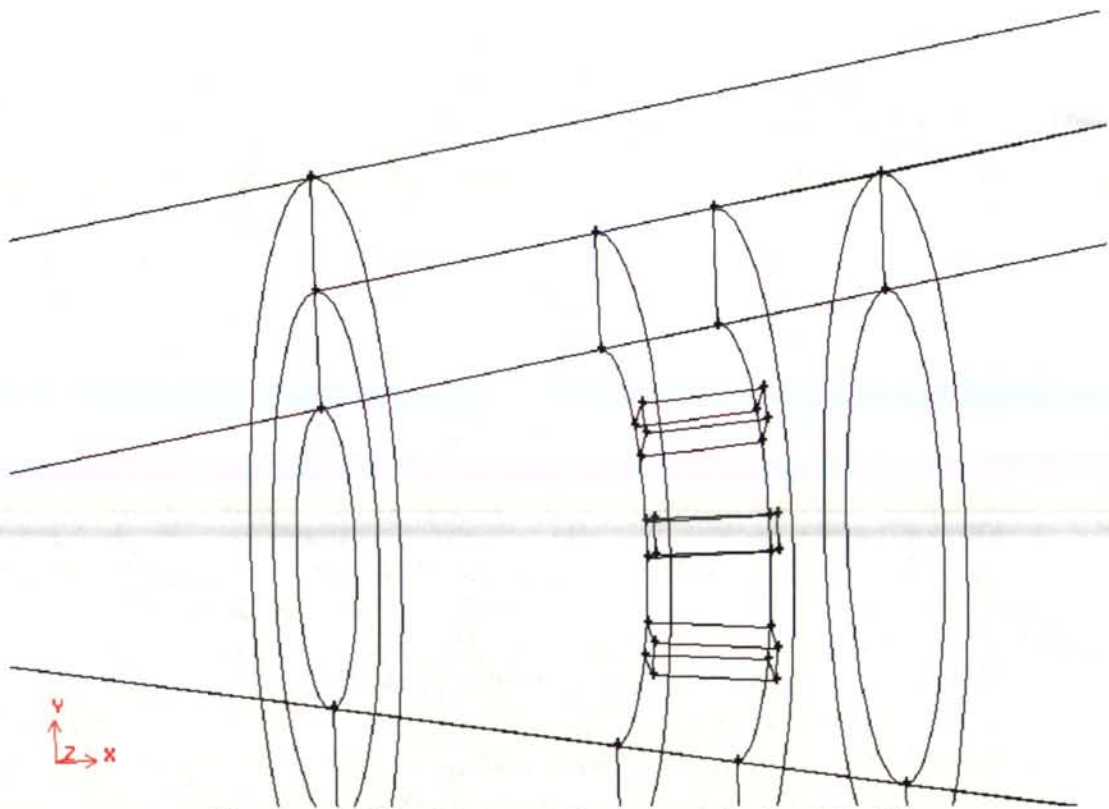


Figure A-4 Block construction around the baseline FE

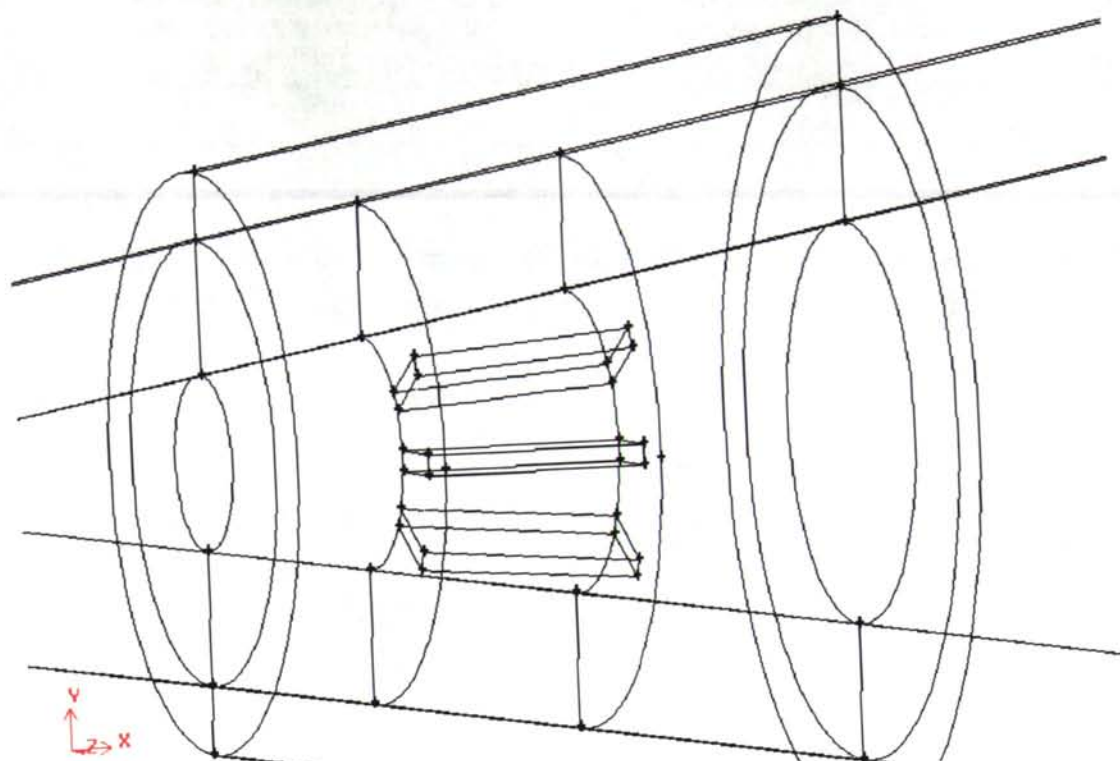


Figure A-5 Block construction around the 3x FE

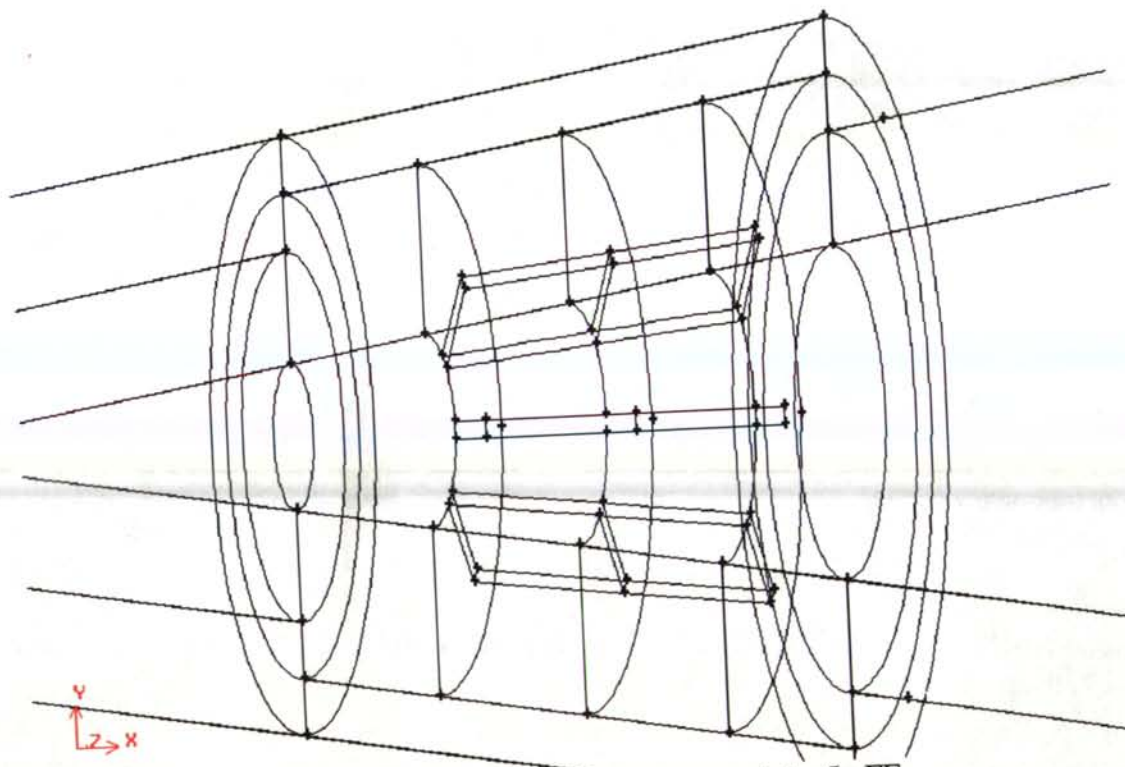


Figure A-6 Block construction around the 5x FE

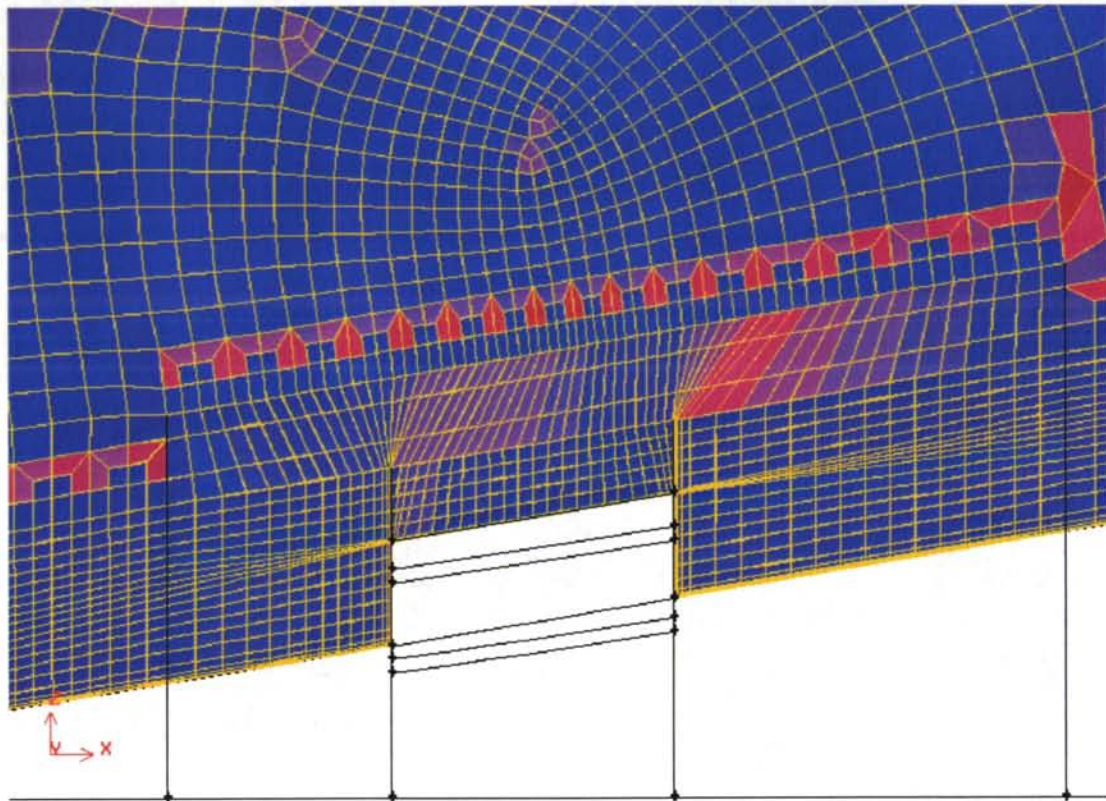


Figure A-7 Mesh cut around the 3x FE in the X-Z plane

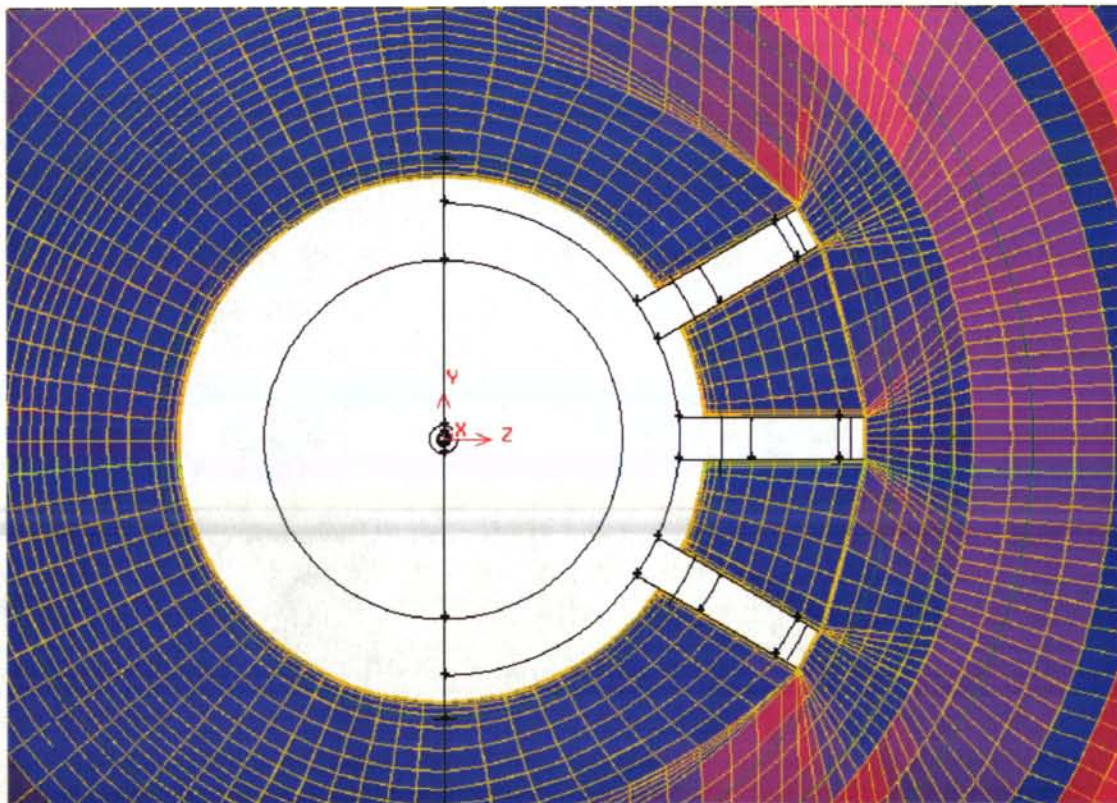
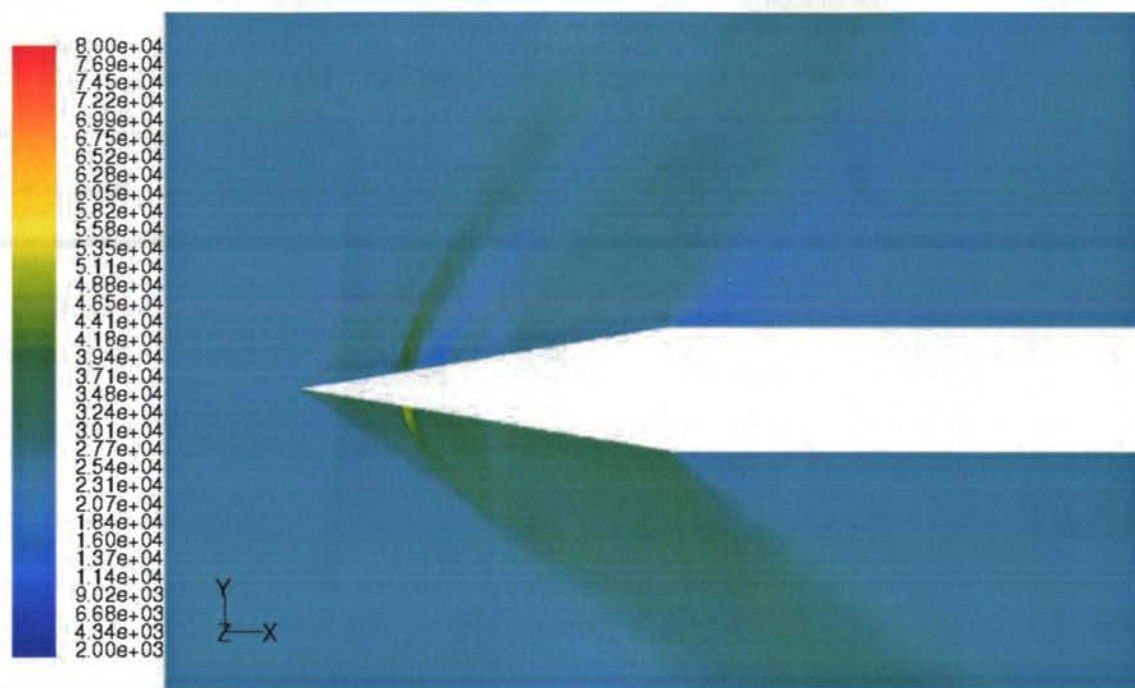


Figure A-8 Mesh cut around the 3x FE in the Y-Z plane

## APPENDIX B

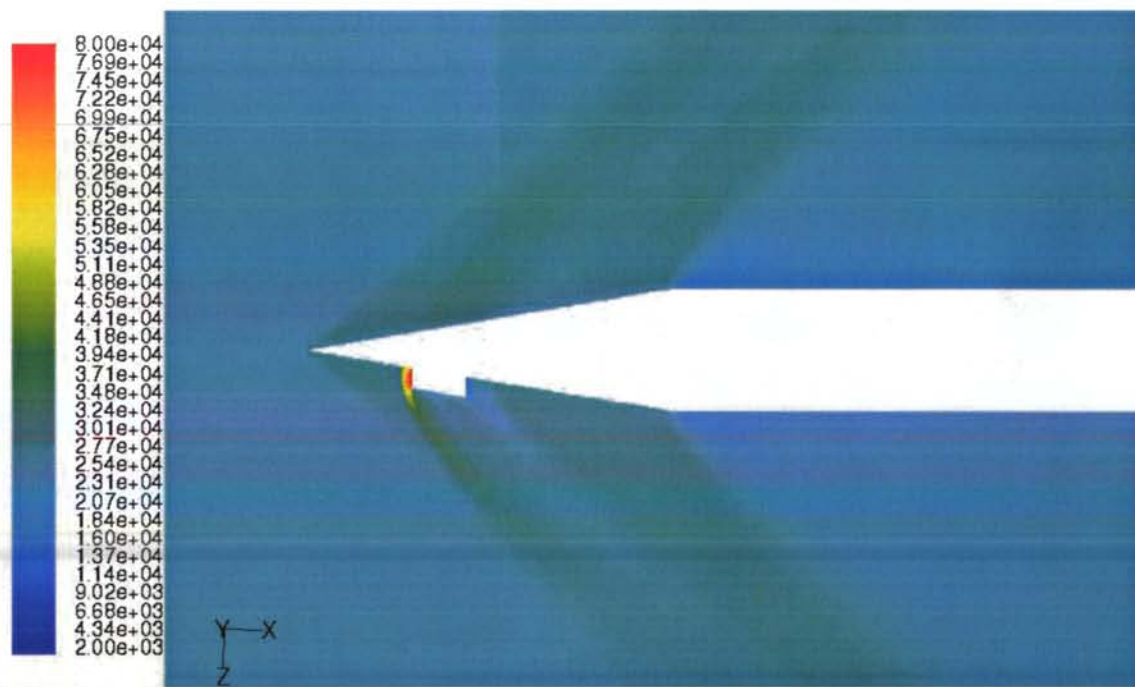
FLUENT™ SOLUTION FIGURES WITH  
RECTANGULAR FLOW EFFECTORS



Contours of Static Pressure (pascal)

Mar 25, 2004  
FLUENT 6.1 (3d, coupled exp, rke)

Figure B-1 Pressure field in the plane of the angle of attack with three 5x FE at 10° AOA



Contours of Static Pressure (pascal)

Mar 25, 2004  
FLUENT 6.1 (3d, coupled exp, rke)

Figure B-2 Pressure field in the plane of the three 5x FE at 10° AOA

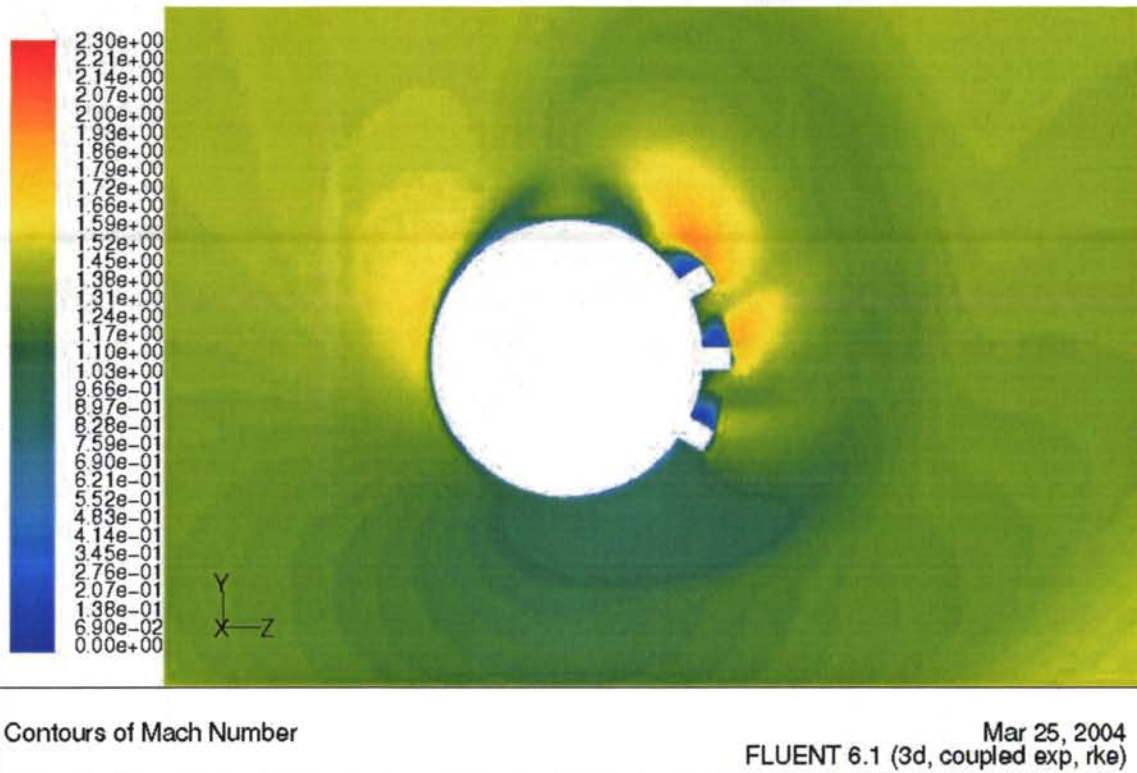


Figure B-3 Mach number around 3 baseline FE with 30 degrees between them with 20° AOA

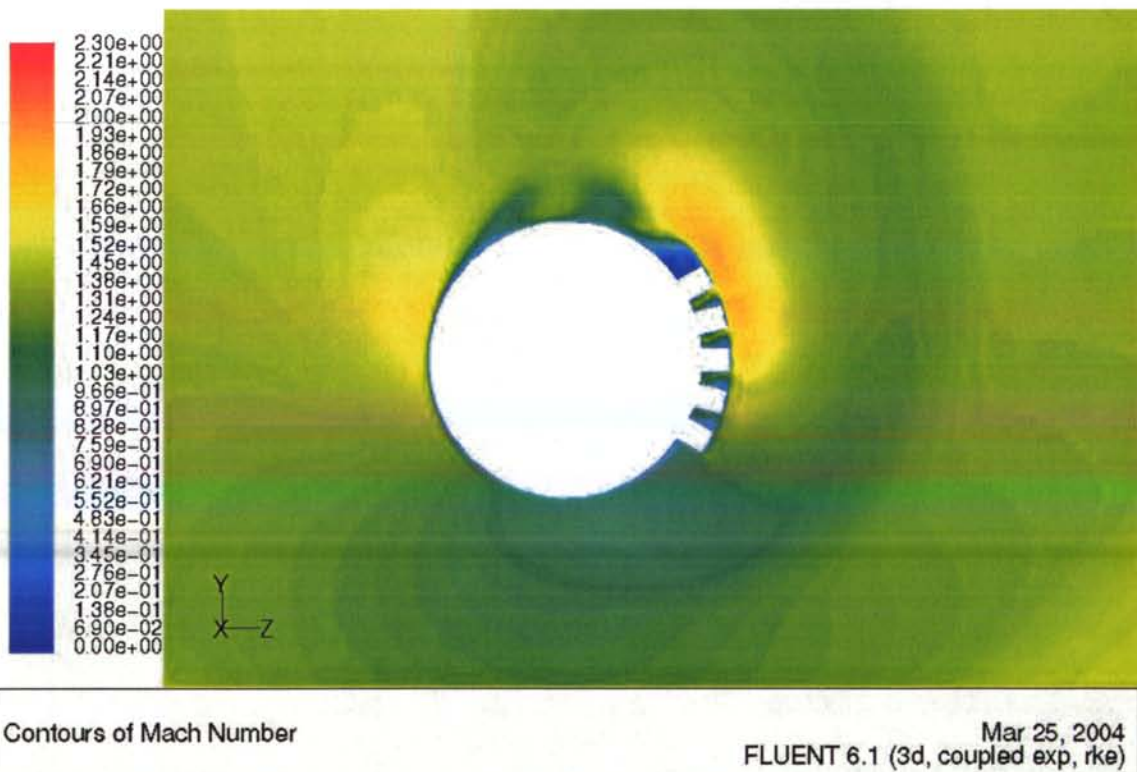
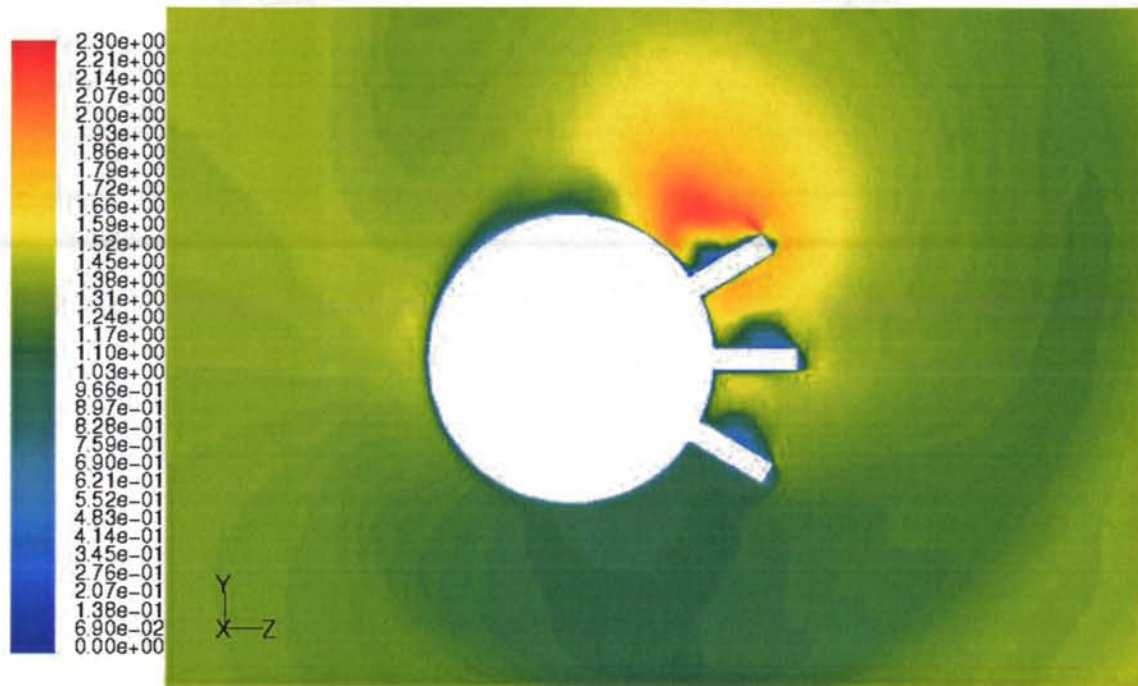


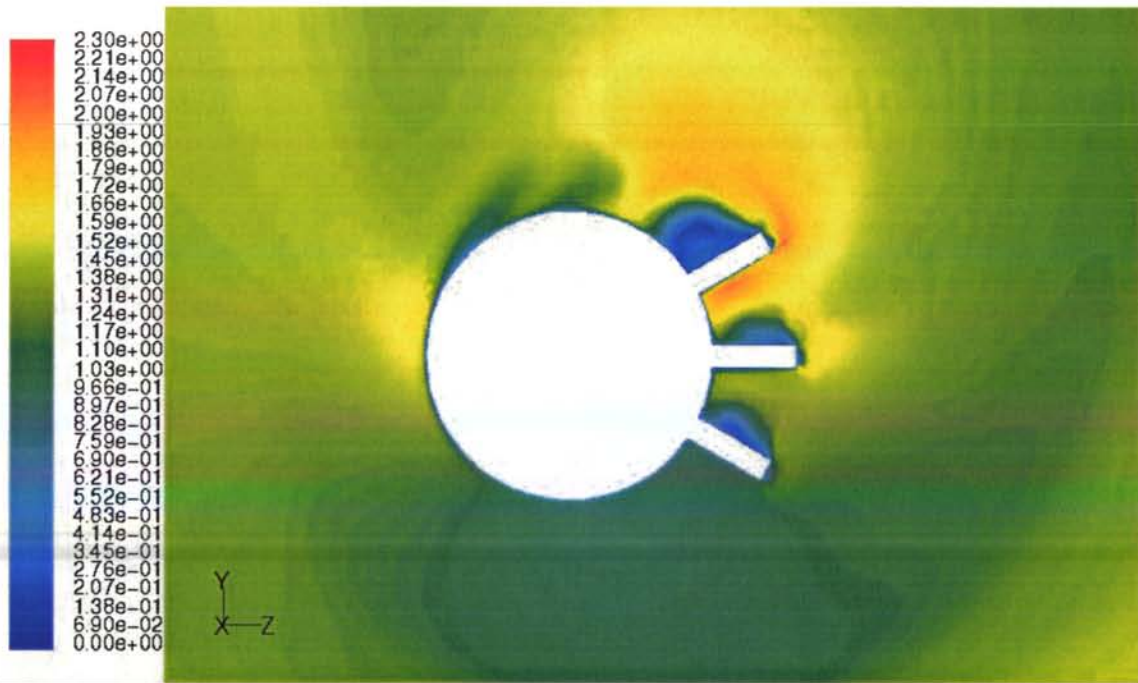
Figure B-4 Mach number around 5 baseline FE with 15 degrees between them with 20° AOA



Contours of Mach Number

Mar 25, 2004  
FLUENT 6.1 (3d, coupled exp, rke)

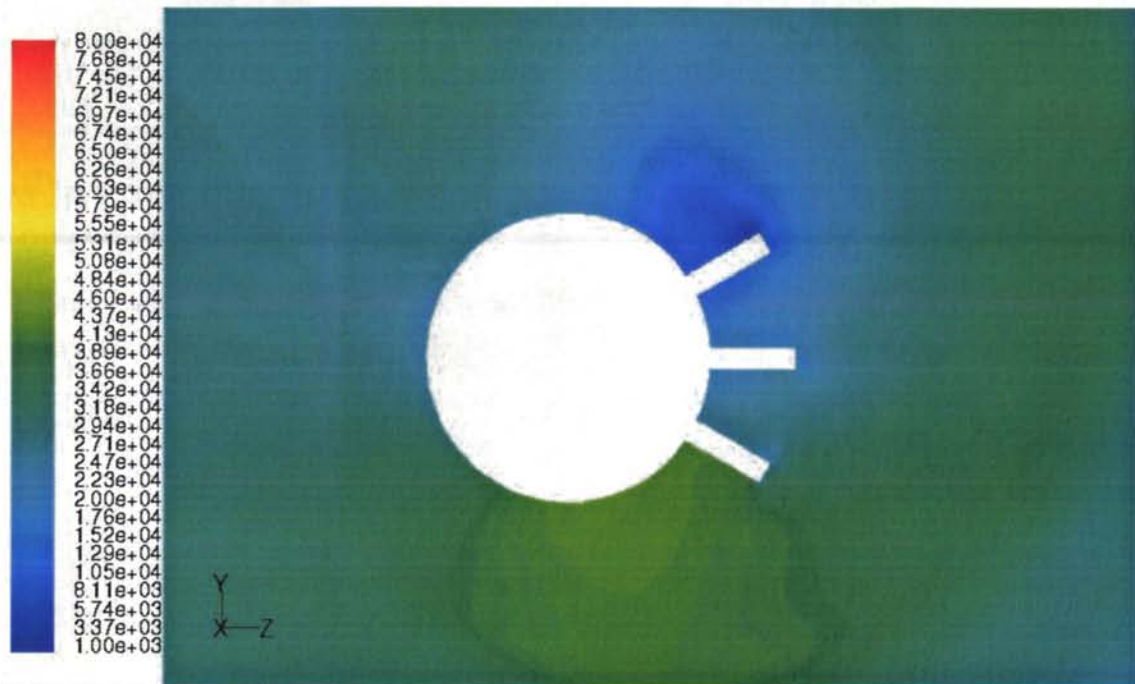
Figure B-5 Mach number around 3 3x FE with 30 degrees between them with 15° AOA



Contours of Mach Number

Mar 25, 2004  
FLUENT 6.1 (3d, coupled exp, rke)

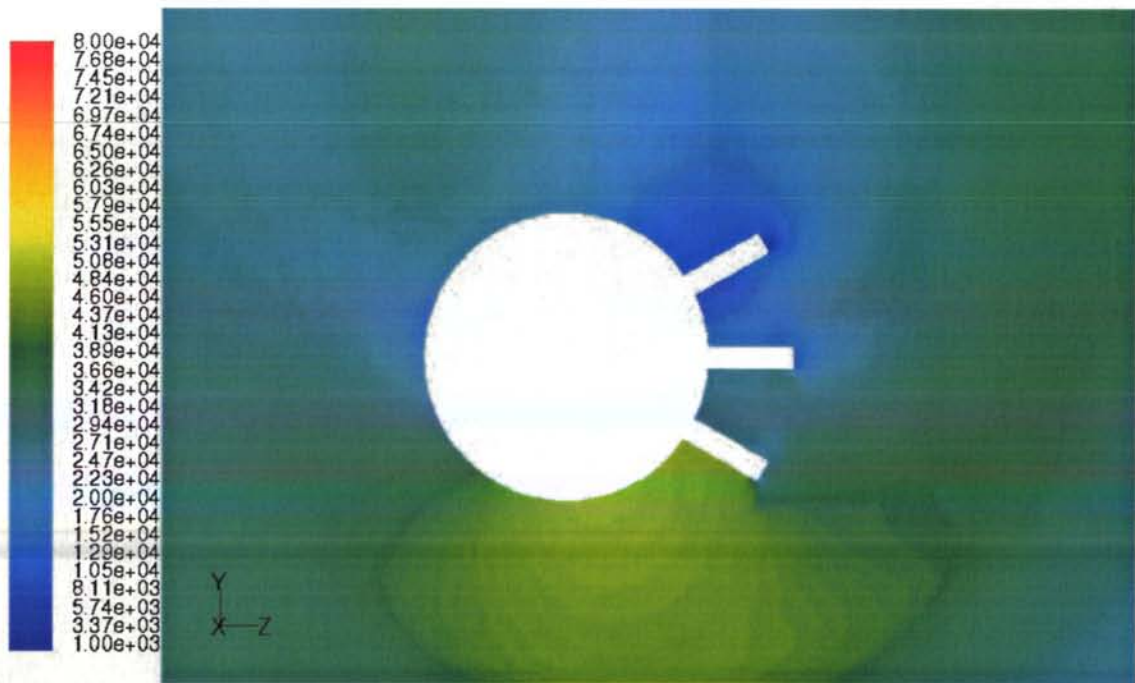
Figure B-6 Mach number around 3 3x FE with 30 degrees between them with 20° AOA



Contours of Static Pressure (pascal)

Mar 25, 2004  
FLUENT 6.1 (3d, coupled exp, rke)

Figure B-7 Pressure around 3 3x FE with 30 degrees between them with 15° AOA



Contours of Static Pressure (pascal)

Mar 25, 2004  
FLUENT 6.1 (3d, coupled exp, rke)

Figure B-8 Pressure around 3 3x FE with 30 degrees between them with 20° AOA

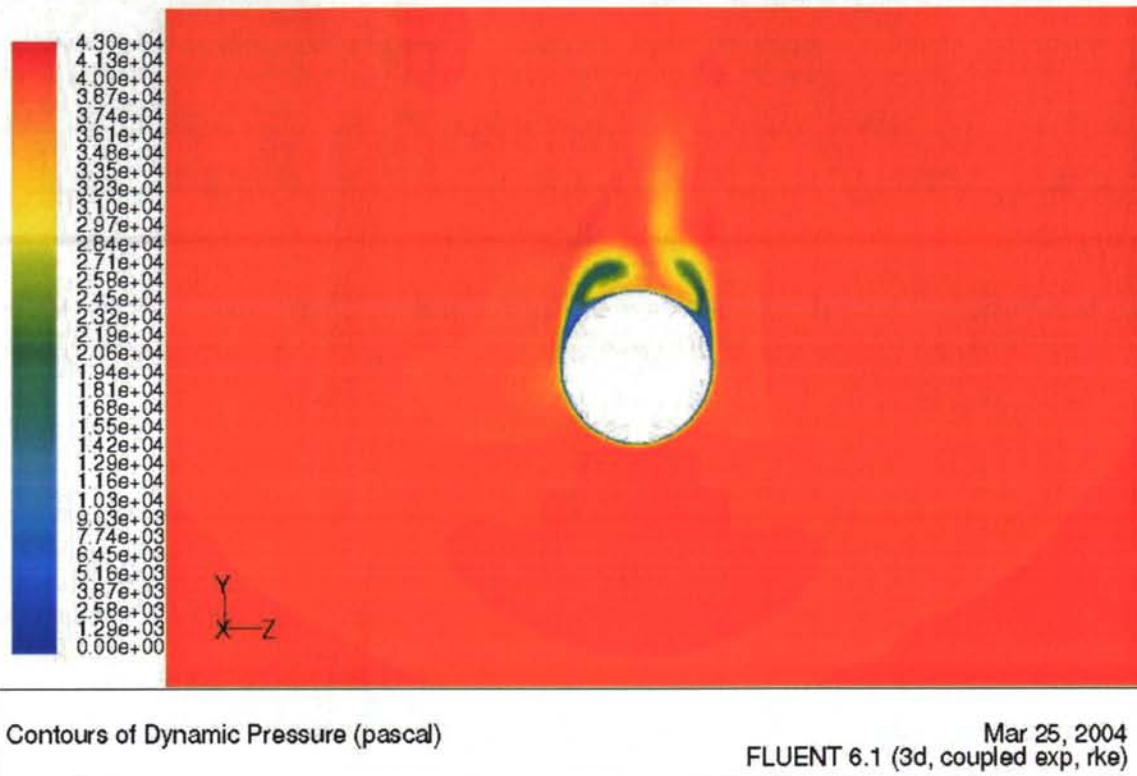


Figure B-9 Dynamic pressure in the middle of the missile (0,2 m) with 15° AOA in the calculation with 3 3x FE having an angle of 30 degrees between them

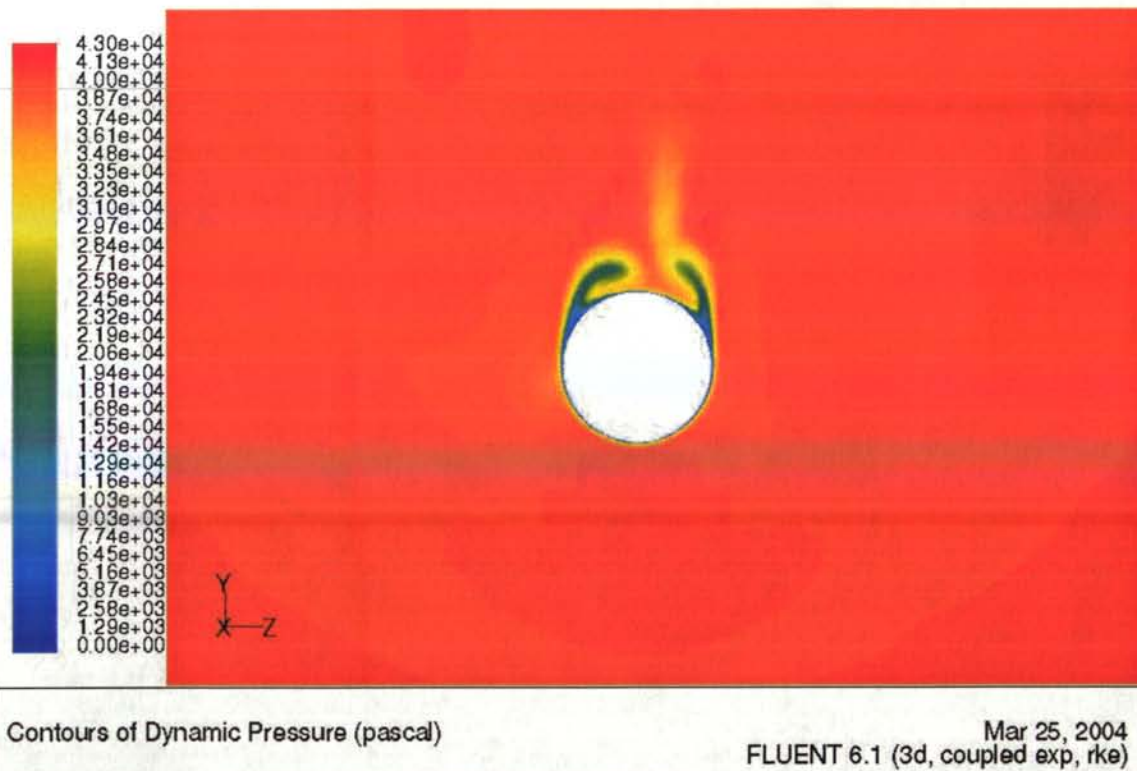


Figure B-10 Dynamic pressure in the middle of the missile (0,2 m) with 20° AOA in the calculation with 3 3x FE having an angle of 30 degrees between them

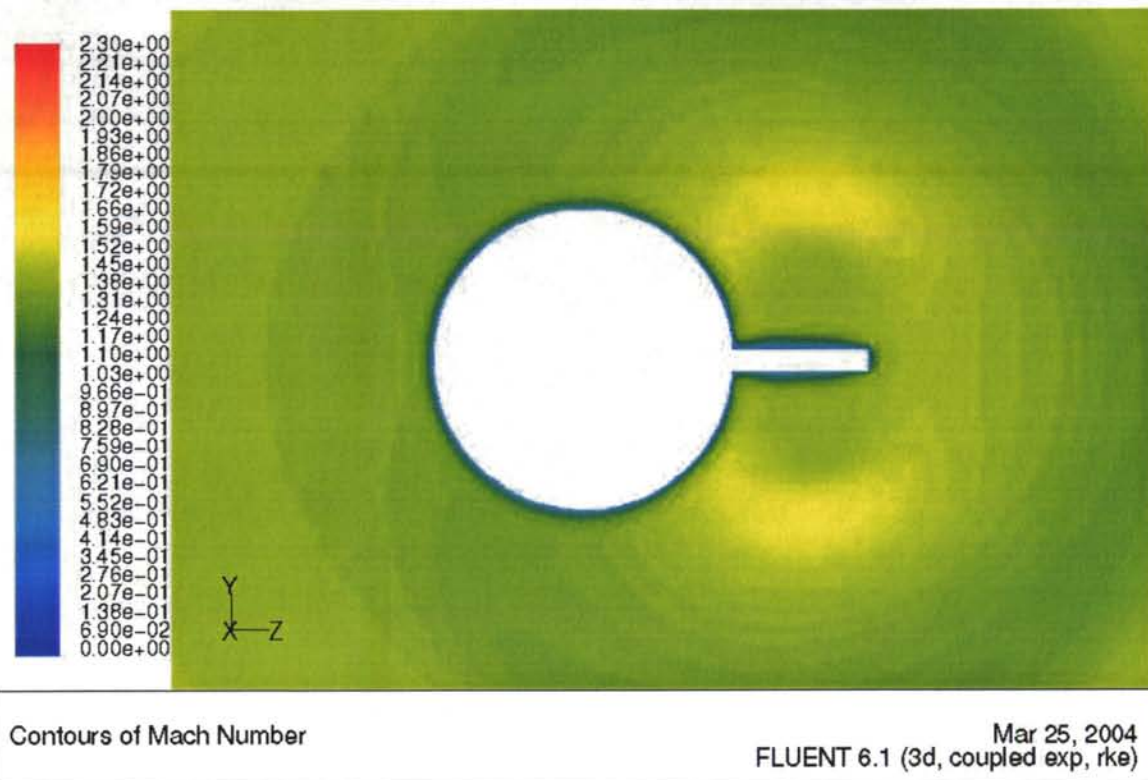


Figure B-11 Mach number around a 5x FE with 0° AOA

## APPENDIX C

GRAPH OF THE PERFORMANCE OF  
RECTANGULAR FLOW EFFECTORS

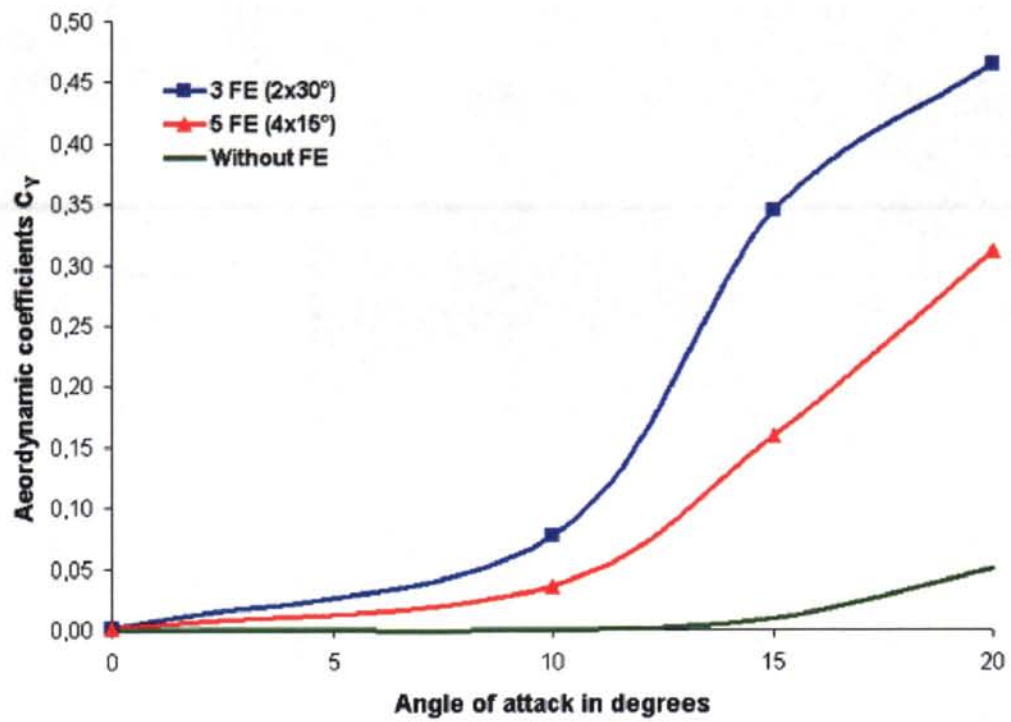


Figure C-1 Graph of the performance of the baseline FE vs the angle of attack

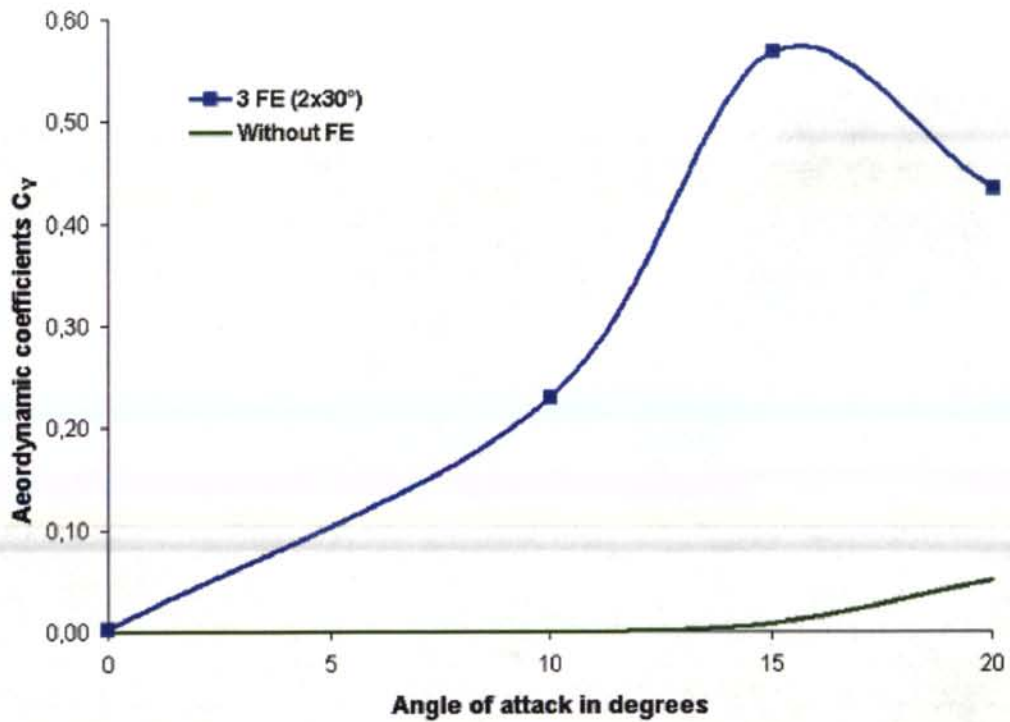


Figure C-2 Graph of the performance of the 3x FE vs the angle of attack

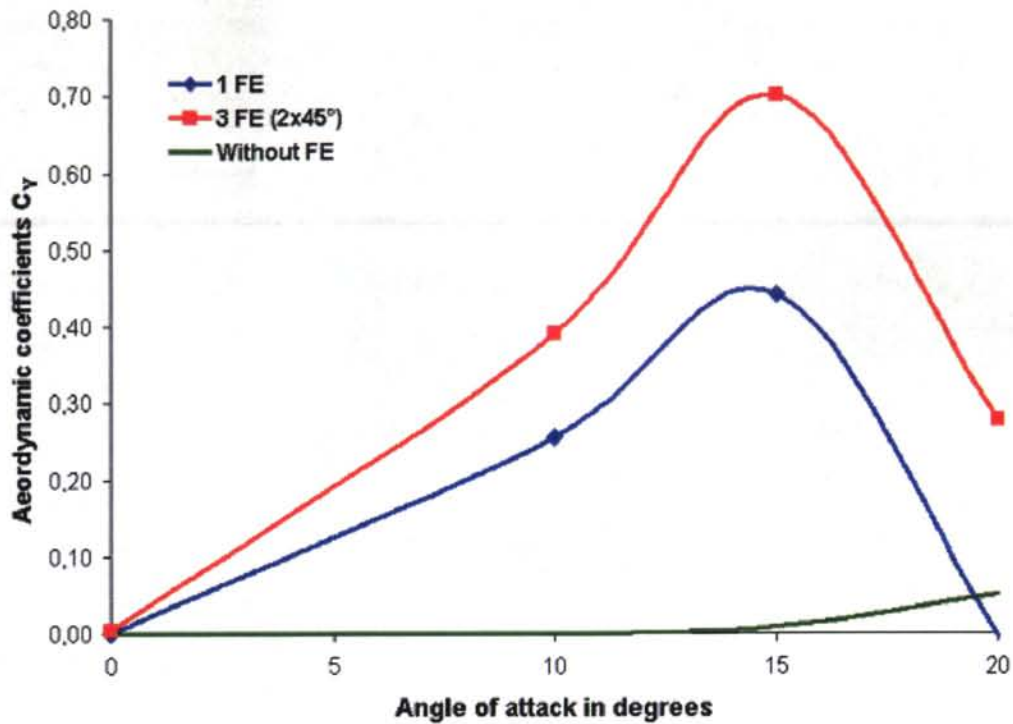


Figure C-3 Graph of the performance of the 5x FE vs the angle of attack

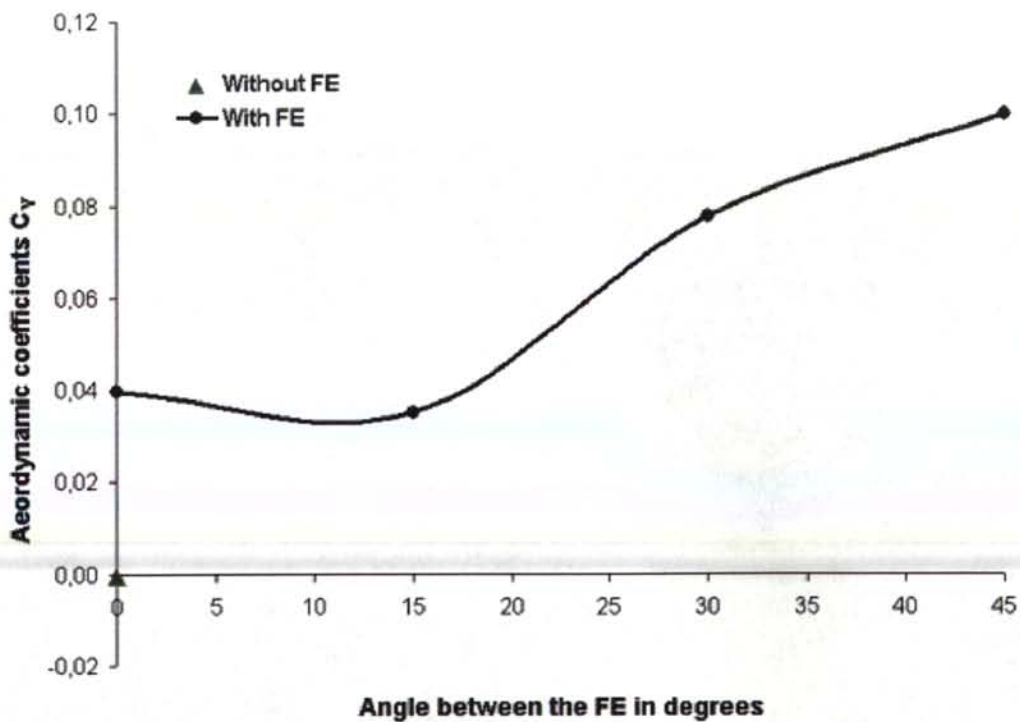


Figure C-4 Graph of the performance of the baseline FE vs the angle between the FE for an angle of attack is 10 degrees. The number of FE is limited to three. With an angle between the devices of zero degrees, there is only one FE.

UNCLASSIFIED/ SANS CLASSIFICATION

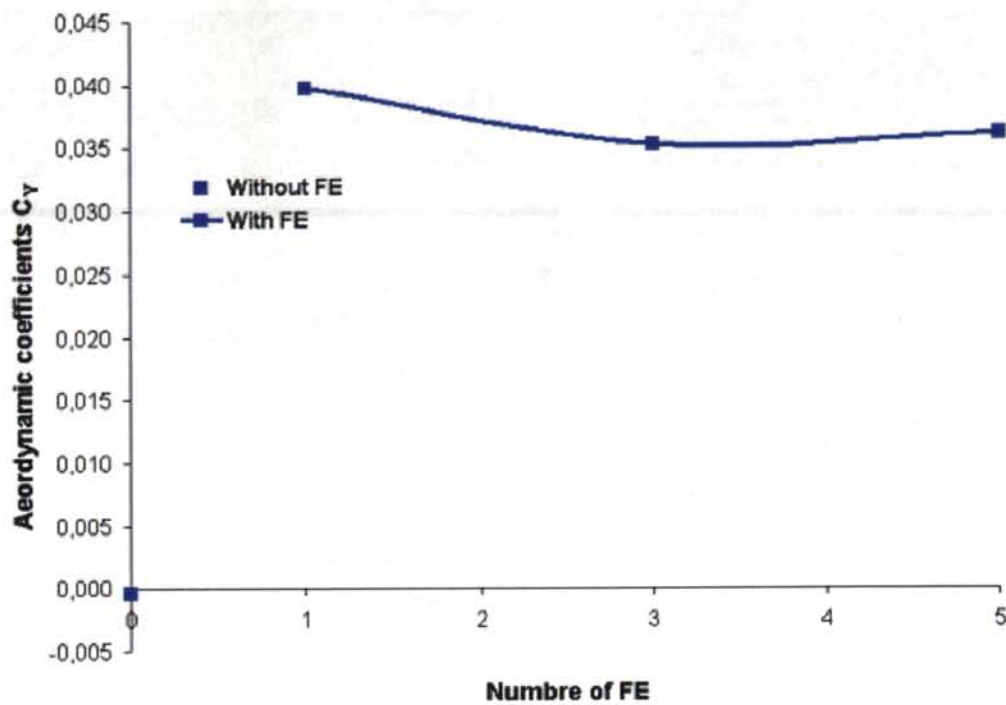


Figure C-5 Graph of the performance of the baseline FE vs the number of FE having an angle of 15 degrees between them and at an angle of attack of 10 degrees

## **Distribution list**

### **INTERNAL DISTRIBUTION**

- 1 - Deputy Director General
- 3 - Document Library
- 1 - F. Wong
- 1 - É. Fournier
- 1 - F. Lesage
- 1 - D. Corriveau
- 1 - N. Hamel (Scientific Authority)
- 1 - C-A. Rabbath

### **EXTERNAL DISTRIBUTION**

- 1 - Director Research and Development Knowledge & Information Management (unbound copy)
- 1 - Director Air Requirement 5
- 1 - Director Science and Technology Air
- 1 - Director Science and Technology Air 4
- 1 - Director Science and Technology Maritime
- 1 - Director Science and Technology Land

- 1 - P. Gosselin (author)
- 1 - P.A. Rainville (author)
  - Numerica Technologies Inc
  - 3420 Lacoste Street
  - Québec, Québec
  - G2E 4P8

- 1 - M. Khalid
- 1 - S. Chen
- 1 - S. McIlwain
  - Institute for Aerospace Research
  - National Research Council of Canada
  - Building U-66
  - 1200 Montreal Road
  - Ottawa, ON
  - Canada
  - K1A 0R6

UNCLASSIFIED  
SECURITY CLASSIFICATION OF FORM  
(Highest Classification of Title, Abstract, Keywords)

DOCUMENT CONTROL DATA		
<b>1. ORIGINATOR</b> (name and address) Defence R&D Canada Valcartier 2459 Pie-XI Blvd. North Val-Bélair, QC G3J 1X8		<b>2. SECURITY CLASSIFICATION</b> (Including special warning terms if applicable) UNCLASSIFIED
<b>3. TITLE</b> (Its classification should be indicated by the appropriate abbreviation (S, C, R or U)) Performance Study for Guidance of a Generic Missile Using Flow Effectors on the Nose		
<b>4. AUTHORS</b> (Last name, first name, middle initial. If military, show rank, e.g. Doe, Maj. John E.) Rainville, Pierre-Antoine, Gosselin, Pierre		
<b>5. DATE OF PUBLICATION</b> (month and year) March 2004	<b>6a. NO. OF PAGES</b> 31	<b>6b. NO. OF REFERENCES</b> 5
<b>7. DESCRIPTIVE NOTES</b> (the category of the document, e.g. technical report, technical note or memorandum. Give the inclusive dates when a specific reporting period is covered.) Contract Report		
<b>8. SPONSORING ACTIVITY</b> (name and address)		
<b>9a. PROJECT OR GRANT NO.</b> (Please specify whether project or grant) 13eg16	<b>9b. CONTRACT NO.</b> W7701-0-2687/001/QCA	
<b>10a. ORIGINATOR'S DOCUMENT NUMBER</b> CR 2004-164	<b>10b. OTHER DOCUMENT NOS</b>  N/A	
<b>11. DOCUMENT AVAILABILITY</b> (any limitations on further dissemination of the document, other than those imposed by security classification)  <input checked="" type="checkbox"/> Unlimited distribution <input type="checkbox"/> Restricted to contractors in approved countries (specify) <input type="checkbox"/> Restricted to Canadian contractors (with need-to-know) <input type="checkbox"/> Restricted to Government (with need-to-know) <input type="checkbox"/> Restricted to Defense departments <input type="checkbox"/> Others		
<b>12. DOCUMENT ANNOUNCEMENT</b> (any limitation to the bibliographic announcement of this document. This will normally correspond to the Document Availability (11). However, where further distribution (beyond the audience specified in 11) is possible, a wider announcement audience may be selected.)		

UNCLASSIFIED  
SECURITY CLASSIFICATION OF FORM  
(Highest Classification of Title, Abstract, Keywords)

UNCLASSIFIED  
SECURITY CLASSIFICATION OF FORM  
(Highest Classification of Title, Abstract, Keywords)

13. ABSTRACT (a brief and factual summary of the document. It may also appear elsewhere in the body of the document itself. It is highly desirable that the abstract of classified documents be unclassified. Each paragraph of the abstract shall begin with an indication of the security classification of the information in the paragraph (unless the document itself is unclassified) represented as (S), (C), (R), or (U). It is not necessary to include here abstracts in both official languages unless the text is bilingual).

Because of the high costs associated with flight and experimental measurements in wind tunnels and test cells, Computational Fluid Dynamics (CFD) is becoming a useful tool for predicting fluid flow. With the recent performance improvements of computers and numerical codes, a much faster prediction of fluid flow, shock wave position and aerodynamic coefficients calculation is believed to be possible allowing the simulations of more complex flow.

This report lies in the continuity of exploring phases on the feasibility to use Flow Effectors for Active Flow Control for the Guidance of Missiles or Rockets. The present study is done on a aerodynamic geometry with a conical nose adapted to the wind tunnel model. Different combinations of rectangular flow effectors place on the nose can have very different characteristics in steady and unsteady operation. Each one of these items has a direct impact on the general performance of the missile. The missile performances can also be affected by flight parameters such as Mach number, altitude and angle of attack.

The aim of this study is to evaluate the performance of an active flow control in the form of a rectangular flow disturber with the aim of controlling a missile or rocket. Using CFD, combinations of different dimensions of flow effectors at different positions on the surface of the missile were evaluated for their impact on overall system performance for a missile flying at Mach 1.5 at an altitude of 6 km from zero to twenty degrees of angle of attack.

14. KEYWORDS, DESCRIPTORS or IDENTIFIERS (technically meaningful terms or short phrases that characterize a document and could be helpful in cataloguing the document. They should be selected so that no security classification is required. Identifiers, such as equipment model designation, trade name, military project code name, geographic location may also be included. If possible keywords should be selected from a published thesaurus, e.g. Thesaurus of Engineering and Scientific Terms (TEST) and that thesaurus-identified. If it is not possible to select indexing terms which are Unclassified, the classification of each should be indicated as with the title.)

Computational Fluid Dynamic, CFD, Flow Effectors, Active Flow Control, MEMS, Microstructure, Missile, Supersonic

UNCLASSIFIED  
SECURITY CLASSIFICATION OF FORM  
(Highest Classification of Title, Abstract, Keywords)

655 hours  
#2214